Cell Reports
Medicine

Article

Impact of physical activity on physical function, mitochondrial energetics, ROS production, and Ca^{2+} handling across the adult lifespan in men

Graphical abstract

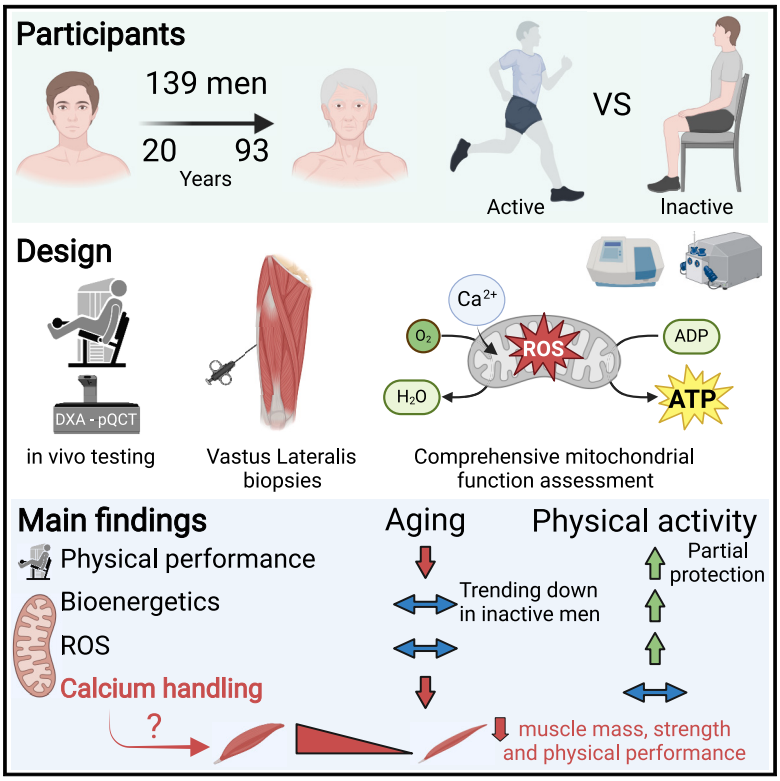

Highlights

- Physical activity helps protect against age-related decline in physical performance
- Physical activity boosts mitochondrial energetics while aging *per se* has no impact
- Mitochondrial ROS production is unaffected by aging in both active and inactive men
- Mitochondrial calcium handling declines with age and is linked to muscle performance

Authors

Marina Cefis, Vincent Marcangeli, Rami Hammad, ..., Richard Robitaille, José A. Morais, Gilles Gouspillou

Correspondence

gouspillou.gilles@uqam.ca

In brief

Cefis et al. show that mitochondrial respiration and ROS production are not affected during healthy muscle aging but identify altered mitochondrial calcium handling as a potential key driving mechanism. They also highlight physical activity as a powerful stimulus to enhance physical performance and mitochondrial energetics throughout the human adult lifespan.

Cefis et al., 2025, Cell Reports Medicine 6, 101968
February 18, 2025
https://doi.org/10.1016/j.xcrm.2025.101968

CellPress

Cell Reports Medicine

CellPress
OPEN ACCESS

Article

Impact of physical activity on physical function, mitochondrial energetics, ROS production, and Ca^{2+} handling across the adult lifespan in men

Marina Cefis,[1,2,3,15] Vincent Marcangeli,[1,2,4,15] Rami Hammad,[1,2,4,5,6] Jordan Granet,[4,5] Jean-Philippe Leduc-Gaudet,[1,7] Pierrette Gaudreau,[8] Caroline Trumpff,[9] Qiuhan Huang,[9] Martin Picard,[9] Mylène Aubertin-Leheudre,[1,2,5] Marc Bélanger,[1,2] Richard Robitaille,[2,10,11] José A. Morais,[2,12,13] and Gilles Gouspillou[1,2,5,14,16,*]

[1]Département des sciences de l'activité physique, Université du Québec À Montréal, Montreal, QC, Canada
[2]Groupe de recherche en Activité Physique Adaptée, Montréal, QC, Canada
[3]INSERM UMR1093-CAPS, UFR des Sciences de santé, Université de Bourgogne, Dijon, France
[4]Département des sciences biologiques, Université du Québec À Montréal, Montreal, QC, Canada
[5]Centre de Recherche de l'Institut Universitaire de Gériatrie de Montréal, Montreal, QC, Canada
[6]Al-Ahliyya Amman university, Faculty of educational sciences, Department of physical and health education, Amman, Jordan
[7]Research Group in Cellular Signaling, Department of Medical Biology, Université du Québec À Trois-Rivières, Trois-Rivières, Canada
[8]Centre de Recherche du Centre Hospitalier de l'Université de Montréal, Département de médecine, Université de Montréal, Montreal, QC, Canada
[9]Division of Behavioral Medicine, Department of Psychiatry, Columbia University Irving Medical Center, and Robert N Butler Columbia Aging Center, Mailman School of Public Health, Columbia University, New York, NY, USA
[10]Département de neurosciences, Université de Montréal, Montreal, QC, Canada
[11]Centre interdisciplinaire de recherche sur le cerveau et l'apprentissage, Montreal, QC, Canada
[12]Research Institute of the McGill University Health Centre, Montreal, QC, Canada
[13]Division of Geriatric Medicine, Faculty of Medicine, McGill University, Montreal, QC, Canada
[14]Meakins-Christie Laboratories, Department of Medicine, McGill University, Montreal, QC, Canada
[15]These authors contributed equally
[16]Lead contact
*Correspondence: gouspillou.gilles@uqam.ca
https://doi.org/10.1016/j.xcrm.2025.101968

SUMMARY

Aging-related muscle atrophy and weakness contribute to loss of mobility, falls, and disability. Mitochondrial dysfunction is widely considered a key contributing mechanism to muscle aging. However, mounting evidence positions physical activity as a confounding factor, making unclear whether muscle mitochondria accumulate bona fide defects with aging. To disentangle aging from physical activity-related mitochondrial adaptations, we functionally profiled skeletal muscle mitochondria in 51 inactive and 88 active men aged 20–93. Physical activity status confers partial protection against age-related decline in physical performance. Mitochondrial respiration remains unaltered in active participants, indicating that aging *per se* does not alter mitochondrial respiratory capacity. Mitochondrial reactive oxygen species (ROS) production is unaffected by aging and higher in active participants. In contrast, mitochondrial calcium retention capacity decreases with aging regardless of physical activity and correlates with muscle mass, performance, and the stress-responsive metabokine/mitokine growth differentiation factor 15 (GDF15). Targeting mitochondrial calcium handling may hold promise for treating aging-related muscle impairments.

INTRODUCTION

One of the most significant changes associated with normal aging is a progressive loss of muscle mass and function.[1–3] These age-related skeletal muscle alterations greatly contribute to reduced functional capacities, mobility impairment, falls, and physical frailty in older adults, dramatically impairing their quality of life.[4,5] Underscoring the magnitude of the impact of aging-related muscle dysfunction, it is estimated that the prevalence of sarcopenia (i.e., the aging-related loss of muscle mass, strength, and function) increases from 14% in 65–70 years old to over 50% in those above 80 years of age,[6] underscoring the need for studies on individuals across the whole adult lifespan. The number of people around the world aged over 60 years was estimated at 1 billion in the year 2020. This figure is expected to be more than double by 2050 (https://www.who.int/health-topics/ageing). Even with a conservative estimate of its prevalence, sarcopenia currently affects over 50 million people and will reach over 200 million in the next 30 years.[6] Furthermore, the direct healthcare costs attributable to sarcopenia and its

sequela are considerable, estimated at 18.5 billion dollars for 2000 alone in the United States,[7] a figure certainly much higher today. Hence, unraveling the mechanisms underlying the aging-related loss of muscle mass and function to promote the development of effective therapeutic interventions is a major challenge in health research.

Among the mechanisms proposed to explain the aging-related alteration in skeletal muscle biology, the accumulation of mitochondrial dysfunction has gained a lot of traction in the past few decades. Impaired mitochondrial function is often depicted as a hallmark of muscle aging, with a reduction in mitochondrial respiration and an increase in mitochondrial reactive oxygen species (ROS) production commonly portrayed as key contributing mechanisms.[8–16] Impaired mitochondrial calcium handling and altered function of the mitochondrial permeability transition pore (mPTP), and potential downstream activation of apoptotic and proteolytic pathways, have also been proposed as potential contributors to skeletal muscle aging.[8,17,18] However, age-related alterations in skeletal muscle mitochondrial biology are not universal findings, and mounting evidence indicates that habitual physical activity is a likely confounding factor when interpreting the impact of aging.[14,15,17,19–23] Most studies conducted in humans also focus on comparisons between young vs. older adults, potentially missing changes that could occur during middle age. Those who did include middle-aged adults mainly focused on mitochondrial bioenergetics (i.e., respiration or ATP production) and did not investigate the impact of habitual physical activity (i.e., by comparing inactive vs. active individuals).[24,25]

To address these gaps in knowledge, we conducted a cross-sectional study in 51 inactive and 88 active men with ages ranging from 20 to 93 years, divided into age groups to tease out when significant changes in parameters may occur. All participants were deeply phenotyped using a comprehensive battery of physical tests. Body and skeletal muscle composition were assessed using dual-energy X-ray absorptiometry (DXA) and peripheral quantitative computed tomography (pQCT), respectively. Vastus lateralis muscle biopsies were performed to assess various aspects of mitochondrial function, including mitochondrial respiration, ROS production (assessed using H_2O_2 emission as a surrogate), and calcium handling, in permeabilized myofibers. Group and correlation analyses were performed to assess the impact of aging and physical activity status on physical performance, mitochondrial bioenergetics, ROS production, and calcium handling.

RESULTS

Baseline participant characteristics

One hundred and thirty-nine men aged from 20 to 93 years old, all living independently in the community and in overall good physical health, were enrolled in the present study. To assess the impact of aging and habitual physical activity, analyses were conducted either by grouping participants according to their age and physical activity status or using age as a continuous variable. For group analyses, participants were divided into the following age groups: young middle age (20–39 year-old[yo]), mature middle age (40–59 yo), young older adults (60–69 yo), and older adults (70+ yo). They were sub-divided into inactive and active subgroups according to their physical activity status (i.e., physically inactive vs. active).

Anthropometric characteristics and body composition data, as well as time spent practicing physical activity, are summarized in Table 1. No effect of aging on body mass was observed (Table 1). An effect of physical activity status on body mass, mainly driven by participants in the 40–59 and 70+ groups, was observed and indicates that, overall, physically active participants had lower body mass compared to their inactive counterparts (Table 1). Body mass index (BMI) significantly increased with aging, an effect attenuated by physical activity status (Table 1). Total fat mass also increased with aging. A significant effect of physical activity status was observed for fat mass indicative of lower fat mass in physically active participants across all age groups (Table 1). Lean mass relative to body mass was significantly reduced with aging. A significant effect of physical activity status was observed for relative lean mass, indicative of higher relative lean mass in physically active participants across age groups (Table 1). In line with data on relative lean mass, absolute lean mass was significantly reduced with aging, although only a trend for an effect of physical activity was observed (Table 1). Aging was associated with a reduction in the number of daily steps (Table 1). By design, daily steps, metabolic equivalent of tasks (MET), and self-reported amount of physical activity were higher in the active participants (Table 1). Details on the type of physical activity (time spent performing aerobic and/or resistance training) performed by all participants are provided in Table 1. No significant impact of aging on overall physical activity, as well as time spent performing aerobic and/or resistance training, was observed in our cohort (Table 1). However, strong trends for a decrease in total physical activity as well as the time spent performing resistance training were noticed in our physically active participants (Table 1).

To further characterize our cohort of participants, various blood biochemical analyses were performed. As shown in Table 1, significant effects of aging and physical activity status were observed for circulating blood glucose concentration assessed in a fasted state, indicative of an increase in fasted glycemia with aging and a lower fasted glycemia in physically active individuals (Table 1). No effect of aging on circulating insulin levels was observed. However, physically active individuals displayed lower circulating insulin levels (Table 1). While no effect of aging was found for the quantitative insulin sensitivity check index (QUICKI) and the homeostatic model assessment of insulin resistance (HOMA-IR), two indexes of whole-body insulin sensitivity, physically active individuals displayed greater QUICKI values and lower HOMA-IR values, both indicative of greater whole-body insulin sensitivity in active participants (Table 1). Circulating fructosamine levels significantly increased with aging, without protection from physical activity status (Table 1). A trend for an increase in total cholesterol with aging was observed, without protection from physical activity status (Table 1). No impact of aging or physical activity status on high-density lipoprotein (HDL) and low-density lipoprotein (LDL) cholesterol was observed. Significant effects of aging and physical activity status on circulating triglycerides levels were observed,

Table 1. Participant characteristics

Groups	20–39 inactive (n = 15)	40–59 inactive (n = 14)	60–69 inactive (n = 9)	70+ inactive (n = 13)	20–39 active (n = 29)	40–59 active (n = 25)	60–69 active (n = 18)	70+ active (n = 16)	Age effect (p value)	PA effect (p value)	Interaction (p value)
General characteristics & body composition											
Age (years)	30.3 ± 4.1	52.1 ± 4.9	64.1 ± 1.5	79.1 ± 7.8	29.7 ± 5.5	49.6 ± 6.9	63.7 ± 2.7	75.9 ± 4.6	<0.001	0.087	0.676
Body mass (kg)	78.3 ± 13.2	87.9 ± 14.8	81.1 ± 12.5	81.5 ± 8.9	78.8 ± 12.0	75.7 ± 10.3	81.0 ± 10.8	76.4 ± 12.7	0.613	0.049	0.105
BMI ($kg.m^{-2}$)	24.2 ± 3.6	28.3 ± 3.5	27.4 ± 3.8	28.6 ± 2.5	25.3 ± 3.7	25.3 ± 3.3	26.7 ± 3.5	25.6 ± 3.3	0.013	0.026	0.033
Fat mass (%)	27.11 ± 7.8	31.7 ± 5.6	29.3 ± 7.2	32.3 ± 5.2	17.8 ± 7.9	21.4 ± 7.3	27.2 ± 7.9	27.2 ± 8.0	<0.001	<0.001	0.117
Lean mass (%)	69.9 ± 7.2	65.6 ± 5.3	68.1 ± 6.7	65.0 ± 4.9	78.6 ± 7.4	75.3 ± 7.0	69.9 ± 7.6	69.7 ± 7.6	<0.001	<0.001	0.111
Lean mass (kg)	54.2 ± 6.9	57.3 ± 8.6	54.6 ± 4.9	52.7 ± 4.4	61.4 ± 7.3	56.6 ± 5.4	56.0 ± 4.7	52.6 ± 5.8	0.007	0.088	0.026
Physical activity level											
Steps per day (n)	5,830 ± 2,107	6,129 ± 2,043	6,781 ± 1,811	3,976 ± 2,276	10,995 ± 4,000	11,743 ± 5,346	8,427 ± 4,394	5,250 ± 2,701	<0.001	<0.001	0.081
METs ($kcal.kg^{-1}.h^{-1}$)	1.39 ± 0.14	1.26 ± 0.14	1.22 ± 0.20	1.07 ± 0.14	1.67 ± 0.36	1.62 ± 0.43	1.31 ± 0.30	1.13 ± 0.22	<0.001	0.001	0.211
Physical activity total ($min.week^{-1}$)	38.3 ± 45.8	37.0 ± 42.9	27.5 ± 55.4	41.8 ± 46.4	635.9 ± 381.9	355.7 ± 288.5	371.1 ± 247.2	377.2 ± 269.8	0.051	<0.001	0.057
Aerobic training ($min.week^{-1}$)	38.3 ± 45.8	32.7 ± 43.4	27.5 ± 55.4	19.6 ± 38.9	413.7 ± 383.9	257.7 ± 260.9	301.1 ± 249.8	220.8 ± 156.8	0.275	<0.001	0.410
Resistance training ($min\ week^{-1}$)	0 ± 0	4.3 ± 16.0	0 ± 0	22.2 ± 35.3	222.2 ± 227.2	97.8 ± 126.8	70.0 ± 78.2	156.4 ± 159.8	0.094	<0.001	0.096
Blood biochemistry											
Glucose ($mmol.L^{-1}$)	5.1 ± 0.6	5.2 ± 0.4	5.8 ± 0.9	5.6 ± 0.7	4.8 ± 0.3	5.0 ± 0.4	5.4 ± 0.8	5.5 ± 1.0	<0.001	0.037	0.928
Insulin ($pmol.L^{-1}$)	61.0 ± 60.4	64.2 ± 37.5	61.6 ± 25.6	52.1 ± 39.4	32.2 ± 20.1	39.0 ± 33.6	48.1 ± 37.1	44.1 ± 22.8	0.817	0.004	0.614
QUICKI	0.35 ± 0.04	0.35 ± 0.03	0.34 ± 0.03	0.35 ± 0.03	0.39 ± 0.05	0.38 ± 0.03	0.38 ± 0.08	0.36 ± 0.03	0.309	<0.001	0.588
HOMA-IR	2.4 ± 2.6	2.5 ± 1.6	2.8 ± 1.5	2.2 ± 1.7	1.2 ± 0.8	1.5 ± 1.3	2.1 ± 2.1	1.8 ± 1.1	0.479	0.005	0.703
Fructosamine ($\mu mol.L^{-1}$)	233.9 ± 26.4	223.6 ± 24.9	235.7 ± 26.7	254.3 ± 35.3	232.1 ± 21.6	229.4 ± 22.8	235.4 ± 34.3	238.5 ± 35.9	0.052	0.565	0.506
Fructosamine per protein ($\mu mol\ l^{-1}.g^{-1}$)	3.2 ± 0.4	3.2 ± 0.4	3.2 ± 0.4	3.7 ± 0.5	3.3 ± 0.3	3.3 ± 0.3	3.4 ± 0.5	3.5 ± 0.4	0.009	0.608	0.434
Total cholesterol ($mmol.L^{-1}$)	4.4 ± 0.8	5.1 ± 1.1	4.9 ± 0.8	4.0 ± 0.9	4.3 ± 0.8	4.8 ± 0.8	4.6 ± 1.0	4.9 ± 0.9	0.057	0.825	0.032
HDL cholesterol ($mmol.L^{-1}$)	1.3 ± 0.2	1.3 ± 0.3	1.4 ± 0.2	1.4 ± 0.4	1.4 ± 0.3	1.5 ± 0.3	1.4 ± 0.3	1.4 ± 0.4	0.654	0.188	0.366
LDL cholesterol ($mmol.L^{-1}$)	2.7 ± 0.7	2.7 ± 0.8	2.9 ± 0.8	2.0 ± 0.7	2.5 ± 0.8	2.7 ± 0.7	2.6 ± 0.8	2.8 ± 0.9	0.343	0.544	0.052
Triglycerides ($mmol.L^{-1}$)	1.0 ± 0.5	2.2 ± 1.4	1.3 ± 0.3	1.3 ± 0.5	1.0 ± 0.4	1.1 ± 0.5	1.1 ± 0.5	1.5 ± 0.7	0.001	0.038	<0.001
C-reactive protein ($mg.L^{-1}$)	1.3 ± 1.4	1.8 ± 1.1	2.6 ± 3.2	1.2 ± 0.7	0.6 ± 0.4	1.5 ± 2.6	1.4 ± 0.9	2.4 ± 3.5	0.164	0.480	0.110
Proteins ($g.L^{-1}$)	72.9 ± 2.8	69.4 ± 2.9	72.6 ± 2.4	69.9 ± 2.9	71.0 ± 2.9	69.2 ± 3.9	68.9 ± 2.9	67.5 ± 4.5	0.001	0.003	0.337
GDF15 ($pg.mL^{-1}$)	361 ± 116	571 ± 136	631 ± 305	1,857 ± 990	329 ± 93	475 ± 99	780 ± 404	1,393 ± 714	<0.001	0.152	0.063

PA, physical activity; BMI, body mass index; METS, metabolic equivalent of tasks; QUICKI, quantitative insulin sensitivity check index; HOMA-IR, homeostatic model assessment for insulin resistance; HDL, high-density lipoprotein; LDL, low-density lipoprotein; GDF15, growth differentiation factor 15. Data are expressed as mean ± SD. $p < 0.05$ was considered statistically significant.

CellPress
OPEN ACCESS

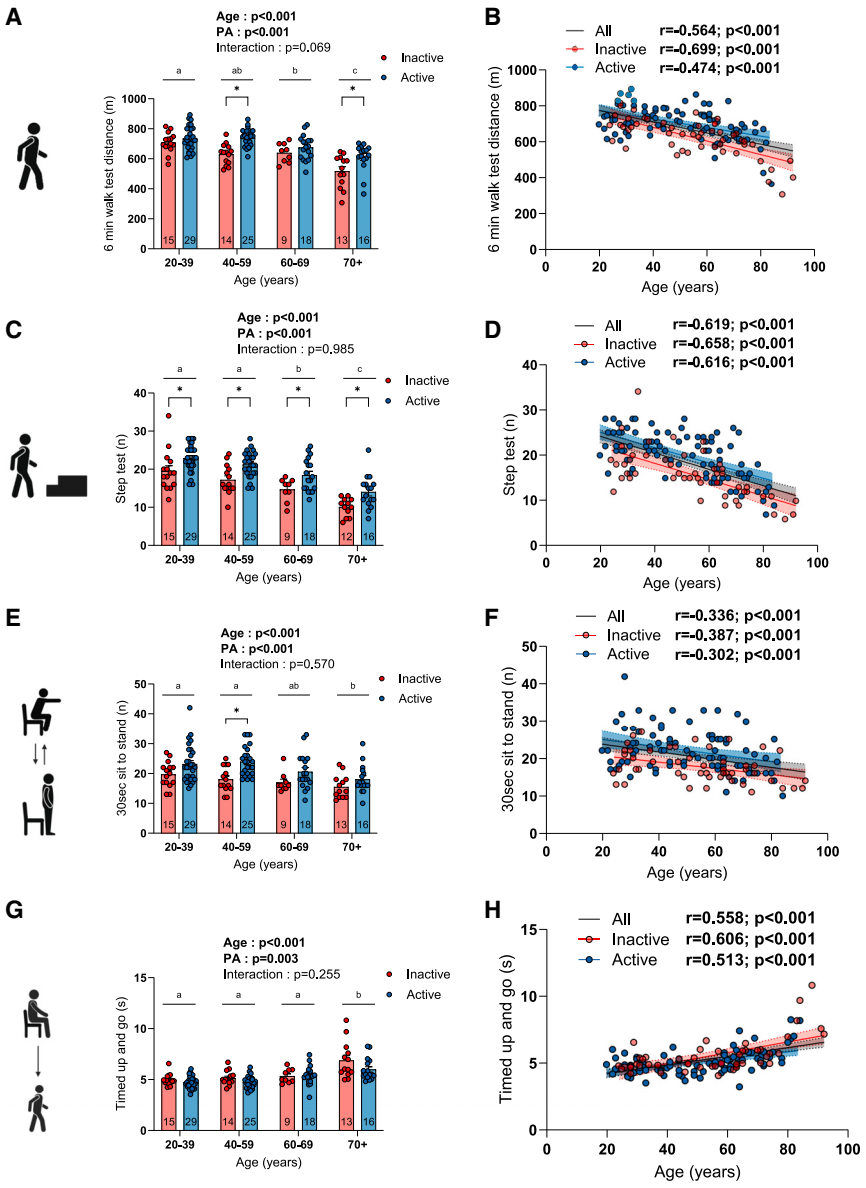

Figure 1. The impact of aging and physical activity status on physical function

Quantification of the performance at the (A and B) 6 min walk test, (C and D) step test, (E and F) sit-to-stand test (number of repetitions performed in 30 s), and (G and H) timed up and go test in inactive and active participants. For group analyses, results of the two-way ANOVA are displayed above each bar graph. Data in bar graphs are presented as mean ± SEM. Tukey *post hoc* tests were performed to test differences between age groups. Differences between inactive and active participants within each age group were assessed using multiple bilateral t tests with false discovery rate (FDR) correction. Groups that do not share the same letter are significantly different. Linear regressions were performed to assess associations between age and variables of interest in the entire cohort (all) and for inactive and active participants separately. Pearson correlation coefficients (r) and *p* values are displayed above each scatterplot. For two-way ANOVA, *post hoc* testing, and regression analyses, $p < 0.05$ was considered statistically significant. For FDR analyses, $q < 0.05$ was considered statistically significant. *, $q < 0.05$. Icons in (A), (C), (E), and (G) were created with BioRender.com. See also Figures S1, S5, S9, and S10.

indicative of an increase in circulating triglyceride levels with aging, with a protection conferred by the physical activity status (Table 1). However, the effect of physical activity seemed mainly driven by the inactive and active participants in the 40–59 groups (Table 1). No effect of aging or physical activity on the circulating levels of C-reactive protein was observed (Table 1). Significant effects of aging and physical activity on the total protein content in serum were observed, indicative of a decrease in total protein content in serum with aging and lower total protein content in active vs. inactive participants (Table 1). Taken altogether, these results indicate that aging is associated with alterations in glucose handling, insulin sensitivity, and triglycerides levels, changes that appear partly prevented by physical activity status. However, it should be noted that the average values displayed in Table 1 for most circulating markers fall well within normal ranges, indicating that both cohorts of inactive and active participants were overall in good general health.

The impact of aging and physical activity status on physical function

All participants underwent a comprehensive battery of tests to assess their physical function. As shown in Figures 1A–1H, performance on the 6-min walk test (Figures 1A and 1B), step test (Figures 1C and 1D), sit-to-stand tests (Figures 1E, 1F, S1A, and S1B), and fast-paced timed up and go (Figures 1G and 1H) was significantly decreased with aging. Significant effects of physical activity status were found for all tested functional capacities, indicating that physically active participants displayed greater functional capacities compared to their inactive counterparts (Figures 1A–1C, 1E, and 1G). Taken altogether, our data show that aging negatively impacts physical function and highlight that physical activity increases physical function in young to older men.

The impact of aging and physical activity status on muscle strength and power

We next evaluated the impact of aging and physical activity status on maximal isometric knee extension strength and maximal lower limb power. As shown in Figures 2A–2D and S1C–S1J, both absolute and relative (to thigh lean mass and body mass) isometric knee extension strength and lower limb extension power were significantly reduced with aging. No significant effect of

CellPress
OPEN ACCESS

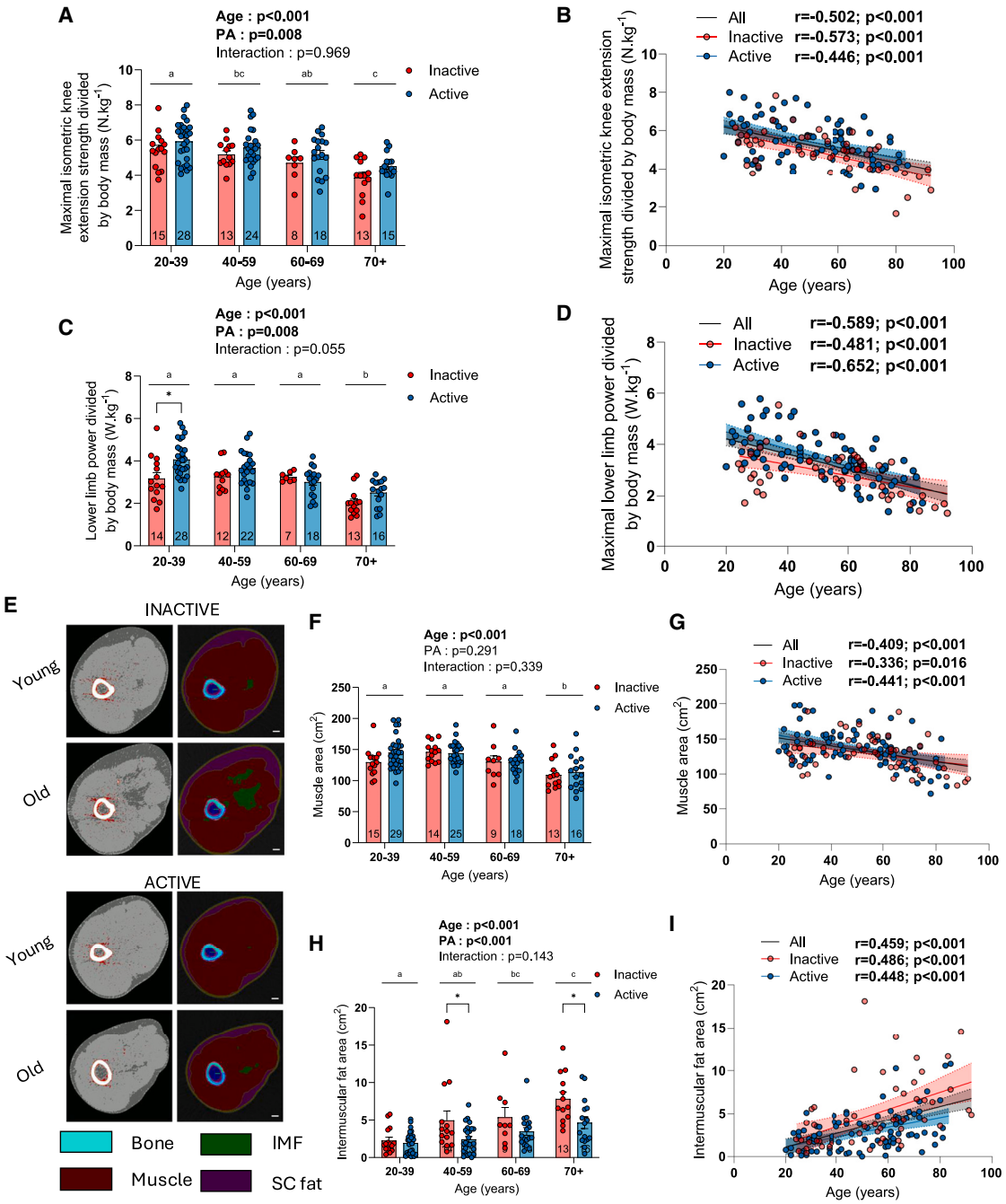

Figure 2. The impact of aging and physical activity status on muscle strength, power, and composition

(A and B) Quantification of the maximal isometric knee extension strength relative to body mass in inactive and active participants.

(C and D) Quantification of the maximal lower limb power relative to body mass in inactive and active participants.

(E) Representative pQCT images of the thigh of young and old inactive and active participants (scale bar: 1 cm).

(F–I) Quantification of the (F and G) muscle cross-sectional area and (H and I) intermuscular fat area in inactive and active participants.

For group analyses, results of the two-way ANOVA are displayed above each bar graph. Data in bar graphs are presented as mean ± SEM. Tukey *post hoc* tests were performed to test differences between age groups. Differences between inactive and inactive participants within each age group were assessed using multiple bilateral t tests with false discovery rate (FDR) correction. Groups that do not share the same letter are significantly different. Linear regressions were performed to assess associations between age and variables of interest in the entire cohort (all) and for inactive and active participants separately. Pearson correlation coefficients (r) and *p* values are displayed above each scatterplot. For two-way ANOVA, *post hoc* testing, and regression analyses, $p < 0.05$ was considered statistically significant. For FDR analyses, $q < 0.05$ was considered statistically significant. *, $q < 0.05$. See also Figures S1, S2, S5, S9, and S10.

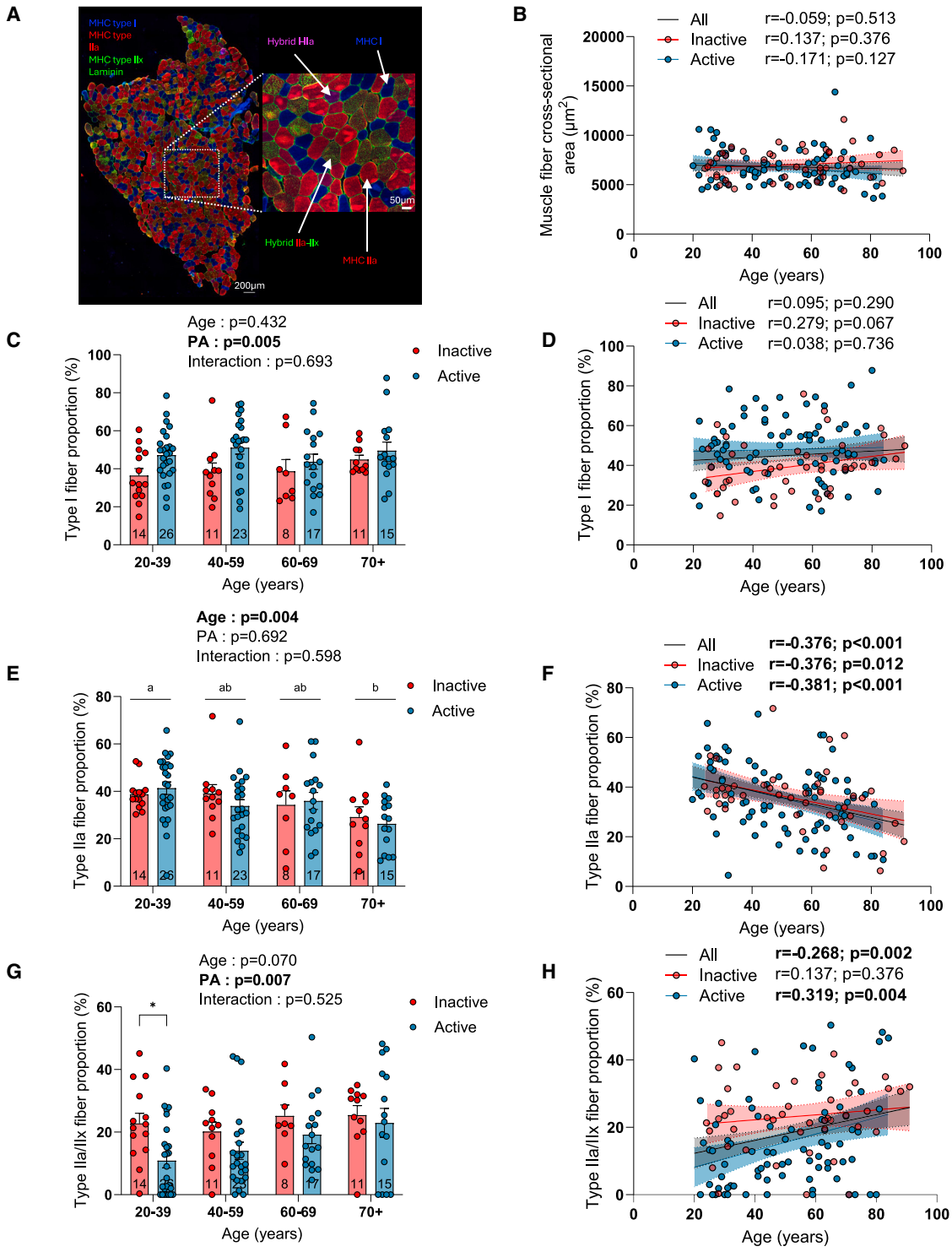

Figure 3. The impacts of aging and physical activity status on muscle fiber type, size, and proportion

(A) Representative triple MHCs (MHC type I: blue; MHC type IIa: red; MHC type IIx: green) and laminin (green) immunolabeling performed on muscle cross-sections (scale bar: 200 µm).

(B) Quantifications of the overall myofiber cross-sectional area in inactive and active participants.

(C–H) Quantification of the proportion of type I (C and D), IIa (E and F), and IIa/IIx (G and H) myofibers in inactive and active participants.

For group analyses, results of the two-way ANOVA are displayed above each bar graph. Data in bar graphs are presented as mean ± SEM. Tukey *post hoc* tests were performed to test differences between age groups. Differences between inactive and active participants within each age group were assessed

(legend continued on next page)

physical activity status on absolute isometric knee extension strength and absolute lower limb extension power was observed (Figures S1C, S1D, S1G, and S1H). Similarly, no significant effect of physical activity status on isometric knee extension strength and lower limb extension power normalized to thigh lean mass was observed (Figures S1E, S1F, S1I, and S1J). However, there were significant physical activity status effects on isometric knee extension strength and relative lower limb extension power normalized to body mass (Figures 2A–2D), indicating greater muscle strength and power relative to body mass in physically active compared to physically inactive individuals. Taken altogether, these data extend the literature showing that muscle strength and power decline with aging and highlight the beneficial effect of physical activity status on muscle strength and power relative to body mass.

The impact of aging and physical activity status on skeletal muscle composition

To gain insight into the impact of aging and physical activity on skeletal muscle mass and composition, images of the thigh were collected using pQCT. Images were acquired at the lower third of the thigh (Figure 2E) and used to quantify muscle area and subcutaneous and intermuscular fat. Segmental analyses of DXA scan images were also performed to assess thigh lean mass. As shown in Figures 2F–2I, muscle area significantly decreased with aging while intermuscular fat area increased. In line with these findings, thigh lean mass assessed using DXA also decreased with aging (Figures S2A–S2D). There was no age effect on subcutaneous fat area in our global population (Figure S2E), although a significant negative correlation was found between age and subcutaneous fat area in inactive participants (Figure S2F). Interestingly, there was no effect of physical activity status on muscle area and thigh lean mass (Figures 2F and S2A). However, there was an effect of physical activity status for intermuscular and subcutaneous fat areas (Figures 2H and S2E), indicative of lower intermuscular and subcutaneous fat in physically active individuals. While young active and inactive participants displayed comparable intermuscular fat, older active groups displayed lower intermuscular fat (Figure 2H), suggesting that physical activity exerts a protective effect against the aging-related increase in intermuscular fat. In contrast, the lower subcutaneous fat content in physically active individuals was mainly explained by lower subcutaneous fat in young active vs. inactive individuals, while older active and inactive individuals displayed comparable subcutaneous fat content (Figure S2E). There was also an effect of physical activity status when thigh lean mass data were expressed relative to body mass, indicating that physically active individuals displayed greater thigh lean mass relative to their overall body mass (Figures S2C and S2D).

A triple myosin heavy chain (MHC) immunolabeling was next performed to assess muscle fiber size and type on vastus lateralis muscle cross-sections (Figures 3A and S3A). As shown in Figure 3B, neither age nor physical activity status affected the overall muscle fiber cross-sectional area (CSA). Data on the impact of aging and physical activity on the fiber type-specific CSA are available in Figures S3B–S3G. No impact of aging was observed for type I, IIa, IIa-IIx, and I-IIa fiber CSA in group analyses (Figures S3B, S3D, and S3F). No impact of physical activity was observed for type I, IIa-IIx, and I-IIa fiber CSA (Figures S3B, S3C, S3F, and S3G). Surprisingly, an overall effect of physical activity was observed for type IIa fibers, indicative of smaller type IIa fibers in active individuals (Figure S3D). Correlation analyses also showed that type IIa fiber CSA decreased with aging only in active participants (Figure S3E). No significant impact of aging was observed for the proportion of type I (Figures 3C and 3D). However, a significant effect of physical activity status was found for the proportion of type I fibers (Figure 3C), indicative of a higher proportion of type I fibers in active individuals. Somewhat in line with data published by Lexell et al.,[26] a trend for an increase in the proportion of type I fibers with age was observed in inactive participants (Figure 3D). However, no such trend was observed in active individuals. Taken altogether, these data on type I fibers suggest that active young individuals display a greater proportion of type I fiber that is not affected by aging. In contrast, inactive young individuals display a lower proportion of type I fibers, which appears to progressively increase with aging. A significant effect of age was observed for the proportion of type IIa fibers, indicative of a progressive decline in the proportion of type IIa fibers with aging (Figures 3E and 3F). No effect of physical activity status on the proportion of type IIa fibers was observed. No pure type IIx fibers were found in the present study, consistent with a recent report indicating that pure type IIx fibers are extremely rare in human skeletal muscles.[27,28] All fibers positive for type IIx MHC also co-expressed type IIa MHC. A trend for an aging effect and a significant physical activity status effect were observed for the proportion of type IIa/IIx fibers in our group analyses (Figure 3G). When analyzed with age as a continuous variable, a significant positive correlation between age and the proportion of type IIa/IIx fibers was observed when all participants were pooled together and when active participants were analyzed separately (Figure 3H). However, no correlation between age and the proportion of type IIa/IIx was found in inactive participants (Figure 3H). Taken altogether, these data suggest that, while young active individuals display a lower proportion of type IIa/IIx fibers vs. inactive individuals, the proportion of these fibers only increases in active participants. No effect of aging nor physical activity status was observed for the proportion of the hybrid type I/IIa fibers (Figure S3H).

The impact of aging and physical activity status on skeletal muscle mitochondrial bioenergetics

As shown in Figure 4A, we prepared permeabilized myofibers from muscle biopsies to perform *ex vivo* high-resolution

using multiple bilateral t tests with false discovery rate (FDR) correction. Groups that do not share the same letter are significantly different. Linear regressions were performed to assess associations between age and variables of interest in the entire cohort (all) and for inactive and active participants separately. Pearson correlation coefficients (r) and *p* values are displayed above each scatterplot. For two-way ANOVA, *post hoc* testing, and regression analyses, $p < 0.05$ was considered statistically significant. For FDR analyses, $q < 0.05$ was considered statistically significant. *, $q < 0.05$. See also Figure S3.

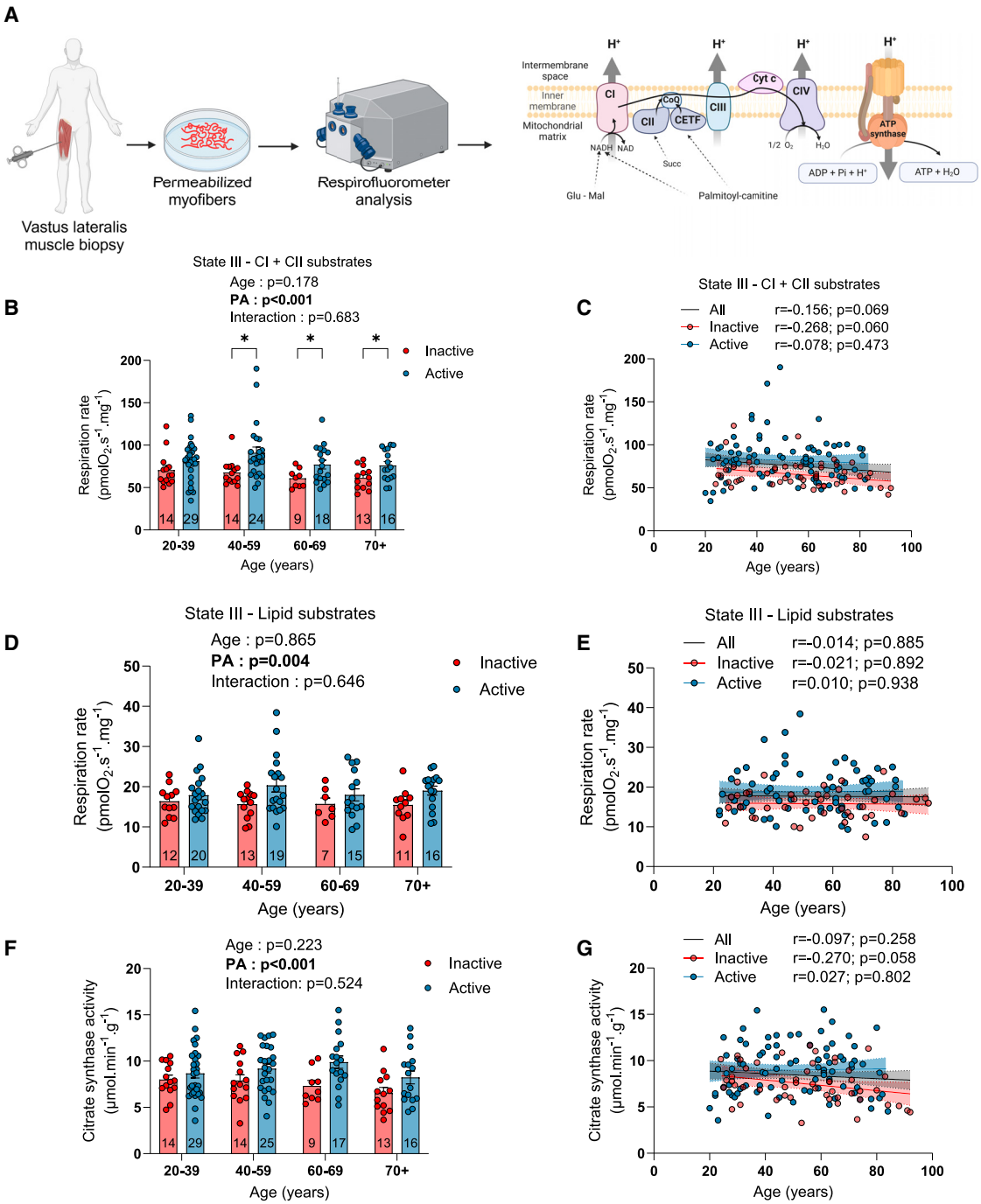

Figure 4. The impact of aging and physical activity status on skeletal muscle mitochondrial respiration and citrate synthase activity

(A) Schematic representation of the experimental design used to assess mitochondrial respiration in permeabilized myofibers.

(B and C) State III (ADP-stimulated) respiration rate driven by complex I and II substrates (glutamate + malate + succinate) in inactive and active participants.

(D and E) State III (ADP-stimulated) respiration rates driven by lipid substrates (palmitoyl-L-carnitine + malate) in inactive and active participants.

(F and G) Citrate synthase activity in inactive and active participants.

For group analyses, results of the two-way ANOVA are displayed above each bar graph. Data in bar graphs are presented as mean ± SEM. Tukey *post hoc* tests were performed to test differences between age groups. Differences between inactive and active participants within each age group were assessed using multiple bilateral t tests with FDR correction. Groups that do not share the same letter are significantly different. Linear regressions were performed to assess

(legend continued on next page)

fluorespirometry analysis to assess mitochondrial respiration. State II respiration rate was evaluated using complex I substrates (glutamate [G] + malate [M]) of the mitochondrial electron transport chain. State II (ADP-restricted) respiration rate supported by complex I substrates was reduced with aging (Figure S4A). Physically active participants displayed higher state II respiration rates compared to their inactive counterparts. In contrast, state III (maximal ADP-stimulated) respiration rates supported by complex I (G + M) and complex I + II substrates (G + M + succinate) were not altered with aging and were significantly higher in active vs. inactive participants (Figures 4B, 4C, and S4B). Interestingly, when data were analyzed with age as a continuous variable, a trend for a decrease in maximal respiration was observed for the overall population and for inactive, but not for active, participants (Figure 4C). In inactive participants, a population for which accelerometers provide reliable estimates of physical activity (accelerometer such as the one used in this study largely underestimates the physical activity of participants engaged in physical activities such as swimming, biking, hockey, or resistance training), a significant positive correlation between the number of daily steps and mitochondrial respiration was observed (Figure S4C). The acceptor control ratio (ACR), an index of the oxidative phosphorylation coupling efficiency (calculated by dividing state III by state II respiration rates), was significantly increased with aging (Figure S4D). No impact of physical activity status on the ACR was observed (Figure S4D).

We also assessed mitochondrial fatty acid oxidation capacity by recording state II and III respiration supported by palmitoyl-L-carnitine (P) and malate. As shown in Figures 4D, 4E, and S4E, neither state II nor state III respiration rates were altered with aging. However, physically active individuals displayed higher respiration rates supported by palmitoyl-L-carnitine and malate compared to their inactive counterparts (Figure 4D, 4E, and S4E). Neither aging nor physical activity status impacted the ACR with P + M substrates (Figure S4F).

To assess whether the greater respiration rates seen in active individuals resulted from a higher mitochondrial content, we assessed citrate synthase (CS) activity, a robust marker of mitochondrial content.[29,30] As shown in Figures 4F and 4G, no effect of aging on CS activity was observed. However, physically active individuals displayed greater CS activity vs. their inactive counterparts (Figure 4F). Similarly to data on maximal respiration, a trend for a decrease in CS activity was observed in inactive participants (Figure 4G). As with the data on respiration, CS activity was positively associated with the number of daily steps in inactive participants (Figure S4G). Importantly, when maximal respiration rates were normalized to CS activity, no effect of aging or physical activity status was observed (Figures S4H and S4I). Collectively, our results indicate that aging *per se* in humans is associated with minimal to no change in mitochondrial respiration and content. They also indicate that physical activity status is associated with greater mitochondrial respiratory capacity and content throughout the human lifespan.

Since multiple previous studies have reported associations between mitochondrial respiration and parameters related to muscle mass, function, and physical performance,[12,25,31] we assessed whether such associations would be found in our cohort. As shown in Figure S5, when all participants were pooled together, mitochondrial respiration was positively associated with muscle CSA, muscle strength, and physical function.

The impact of aging and physical activity status on skeletal muscle mitochondrial ROS production

Mitochondrial H_2O_2 emission (a widely used surrogate of mitochondrial ROS emission) was assessed in permeabilized myofibers using the Amplex UltraRed system (Figure 5A). As illustrated in Figures 5B–5E and S6A–S6D, neither state II nor state III H_2O_2 emission rates supported by complex I or complex I and II substrates were affected by aging. The maximal H_2O_2 emission rate measured after the addition of oligomycin (ATP synthase inhibitor) and antimycin A (complex III inhibitor) was not impacted by aging (Figures 5D and 5E). Importantly, in all conditions tested, physically active participants displayed higher rates of H_2O_2 emission compared to inactive participants (Figures 5B–5E). No impact of aging or physical activity status on state II and state III H_2O_2 emission rates supported by lipid substrates (palmitoyl-L-carnitine and malate) was observed (Figures 5F, 5G, S6E, and S6F). To assess whether aging and/or physical activity status impact intrinsically mitochondrial H_2O_2 emission rates, the free radical leak was quantified by normalizing H_2O_2 emission to oxygen consumption rates. As can be seen in Figure S7, no impact of aging or physical activity status on mitochondrial free radical leak generation was observed. H_2O_2 emission rates were also normalized to a marker of mitochondrial content, CS activity. As shown in Figure S8, no impact of aging or physical activity status on mitochondrial H_2O_2 emission rates normalized to CS activity was observed in group analyses. Correlation analyses revealed that aging in inactive participants was associated with an increase in H_2O_2 emission rates normalized to CS activity in state II and state III supported by complex I substrates (Figures S8B and S8D). However, no such association was found for H_2O_2 emission rates normalized to CS activity in state III supported by complex I and II substrates or for maximal H_2O_2 production induced by antimycin A (Figures S8F and S8H). No negative association was observed between mitochondrial H_2O_2 emission and indices of physical function, strength, and muscle mass (Figures S9 and S10). Taken together, our results indicate that aging *per se* in humans is not associated with an increase in the rate of mitochondrial H_2O_2 emission. They also indicate that being physically active results in greater H_2O_2 emission rates, an effect likely explained by a higher mitochondrial content in active individuals. Lastly, they indicate that intrinsic alterations in mitochondrial H_2O_2 emission are unlikely to contribute to the aging-related loss of muscle mass and function in humans.

associations between age and variables of interest in the entire cohort (all) and for inactive and active participants separately. Pearson correlation coefficients (r) and *p* values are displayed above each scatterplot. For two-way ANOVA, *post hoc* testing, and regression analyses, $p < 0.05$ was considered statistically significant. For FDR analyses, $q < 0.05$ was considered statistically significant. *, $q < 0.05$. (A) was created with BioRender.com. See also Figures S4, S5, S7, and S13.

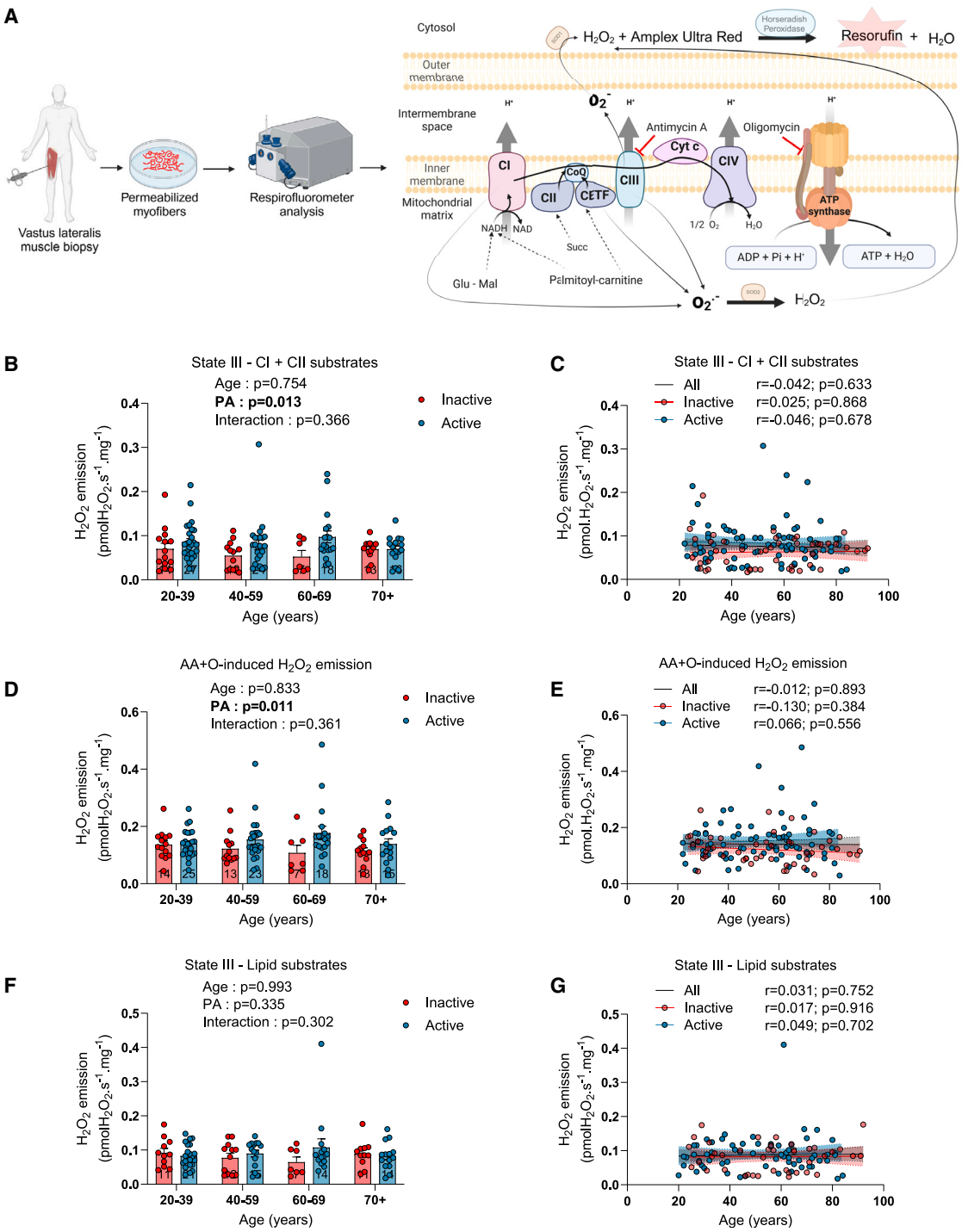

Figure 5. The impact of aging and physical activity status on skeletal muscle mitochondrial H_2O_2 emission

(A) Schematic representation of the experimental design used to assess mitochondrial H_2O_2 emission in permeabilized myofibers.

(B and C) State III H_2O_2 emission rates driven by complex I and II substrates (glutamate + malate + succinate) in inactive and active participants.

(D and E) Maximal H_2O_2 emission rates induced by the addition of antimycin A (AA) and oligomycin (O) in the presence of complex I and II substrates in inactive and active participants.

(F and G) State III H_2O_2 emission rates driven by lipid substrates (palmitoyl-L-carnitine + malate) in inactive and active participants.

For group analyses, results of the two-way ANOVA are displayed above each bar graph. Data in bar graphs are presented as mean ± SEM. Tukey *post hoc* tests were performed to test differences between age groups. Differences between inactive and active participants within each age group were assessed using multiple bilateral t tests with FDR correction. Groups that do not share the same letter are significantly different. Linear regressions were performed to assess

(legend continued on next page)

The impact of aging and physical activity status on skeletal muscle mitochondrial calcium handling

The impact of aging and physical activity status on mitochondrial calcium handling remains an understudied aspect of mitochondrial biology in humans. In the present study, mitochondrial calcium handling was assessed in permeabilized phantom myofibers[17,32] by exposing mitochondria to a saturating calcium challenge. Such an approach allows the measurement of the mitochondrial calcium retention capacity (mCRC), of the time to mPTP opening, and of the mitochondrial calcium uptake rate (Figure 6A). The time to pore opening and mCRC were significantly reduced by aging (Figures 6B–6D, S11A, and S11B). *Post hoc* analyses for the mCRC showed that this reduction was significant between the 20–39 and 70+ and between the 60–69 and 70+ groups. Physical activity status had no impact on mCRC or time to pore opening (Figures 6B and 6C). As suggested by our ANOVA and *post hoc* analyses, further examinations of the relationship between aging and mCRC and the time to mPTP opening revealed that, while both parameters were quite stable from 20 to 60 years of age, both sharply declined after 60 (Figures S11A and S11B). Interestingly, mCRC was correlated with markers of physical performance and muscle mass and function such as thigh lean mass, knee extension strength, and the performances at the 6 min walk test and step test (Figures 6E–6H). A trend for a positive correlation between mCRC and muscle CSA was also observed when all participants were pooled together (Figure S11C). No impact of aging on the mitochondrial calcium uptake rate was found in our cohort (Figure S12). A trend for a higher calcium uptake rate in our physically active participants, mainly driven by participants aged 40 and over, was observed in our group analyses (Figure S12A). Altogether, our data indicate that mitochondrial calcium handling is altered with aging independently from physical activity status and highlight positive associations between mCRC and muscle strength and physical performance.

Association between various aspects of mitochondrial function and the stress-responsive metabokine/mitokine GDF15

Growth differentiation factor 15 (GDF15) has been described as a stress-responsive metabokine, which is particularly increased in response to mitochondrial stress and dysfunction and is often referred to as a mitokine.[33–35] GDF15 has also recently emerged as a potential key player in the human aging process (see Conte et al.[34] for a detailed review). Here, we investigated whether specific aspects of mitochondrial biology in our cohort were associated with plasma GDF15 levels. As can be seen in Figures S13A and S13B and Table 1, plasma GDF15 levels were exponentially and strongly correlated with age ($r = 0.83$, $p < 0.0001$) in the whole cohort and in active and inactive individuals separately. This confirms previous reports that have positioned GDF15 as a biomarker of human aging.[36–38] Since the relationship between aging and plasma GDF15 levels was not linear (i.e., the aging-related increase in plasma GDF15 levels seemed to accelerate after 60), and because GDF15 values were not normally distributed on our cohort, log-transformed GDF15 values were used in regression analyses. Across the whole cohort, we found that individuals with higher plasma GDF15 levels had lower maximal mitochondrial respiratory capacity, a correlation that was stronger and only significant among inactive participants (Figure S13C). No association between state III (ADP-stimulated) mitochondrial respiration driven by lipid substrates and plasma GDF15 levels could be observed (Figure S13D). No association between mitochondrial H_2O_2 emission and plasma GDF15 levels could be found (Figures S13E and S13F). However, individuals with higher levels of GDF15 had mitochondria more susceptible to undergo permeability transition (Figure 6I). Taken altogether, these data relate skeletal muscle mitochondrial respiration and calcium handling to the systemic aging marker plasma GDF15.

DISCUSSION

While impairments in mitochondrial function are often portrayed as causally involved in the aging-related loss of muscle mass and function, evidence has emerged in the past few decades positioning physical activity as a major confounder.[19,20,39] Until now, much of the research effort has been focused on mitochondrial respiration and ROS production while other important mitochondrial functions, such as calcium handling, have been understudied in humans. To disentangle the relationship between aging, multiple aspects of mitochondrial function, and physical activity in humans, we evaluated physical function, muscle mass and performance, muscle phenotype, and various aspects of mitochondrial function in 51 inactive and 88 active men from 20 to 93 years of age. Our data revealed that physical performance declines with age, with partial protection from physical activity. While a trend for reduced maximal mitochondrial respiration was observed in inactive participants, no impact of aging was observed in active participants, indicating that aging *per se* does not alter mitochondrial respiration. Similarly, fatty acid (palmitoyl-carnitine)-supported respiration was not altered by aging. Our data also indicate that physically active participants displayed higher fatty acid-supported respiration as well as maximal respiration across the adult lifespan. Mitochondrial ROS production was unaffected by aging, and physically active participants even displayed higher ROS production. Negative associations between mitochondrial ROS production and muscle mass, function, or physical performance were not seen, indicating that mitochondrial ROS overproduction is unlikely to play a role in the muscle aging process. In contrast, mCRC and time to mPTP opening decreased with aging regardless of the physical activity status. mCRC also correlates with muscle strength and performance. Hence, based on our data, we posit that alterations in mitochondrial calcium handling may be a potential driver of muscle aging and that targeting mitochondrial calcium handling and/or

associations between age and variables of interest in the entire cohort (all) and for inactive and active participants separately. Pearson correlation coefficients (r) and *p* values are displayed above each scatterplot. For two-way ANOVA, *post hoc* testing, and regression analyses, $p < 0.05$ was considered statistically significant. For FDR analyses, $q < 0.05$ was considered statistically significant. *, $q < 0.05$. AA, antimycin A; O, oligomycin. (A) was created with BioRender.com. See also Figures S6–S10 and S13.

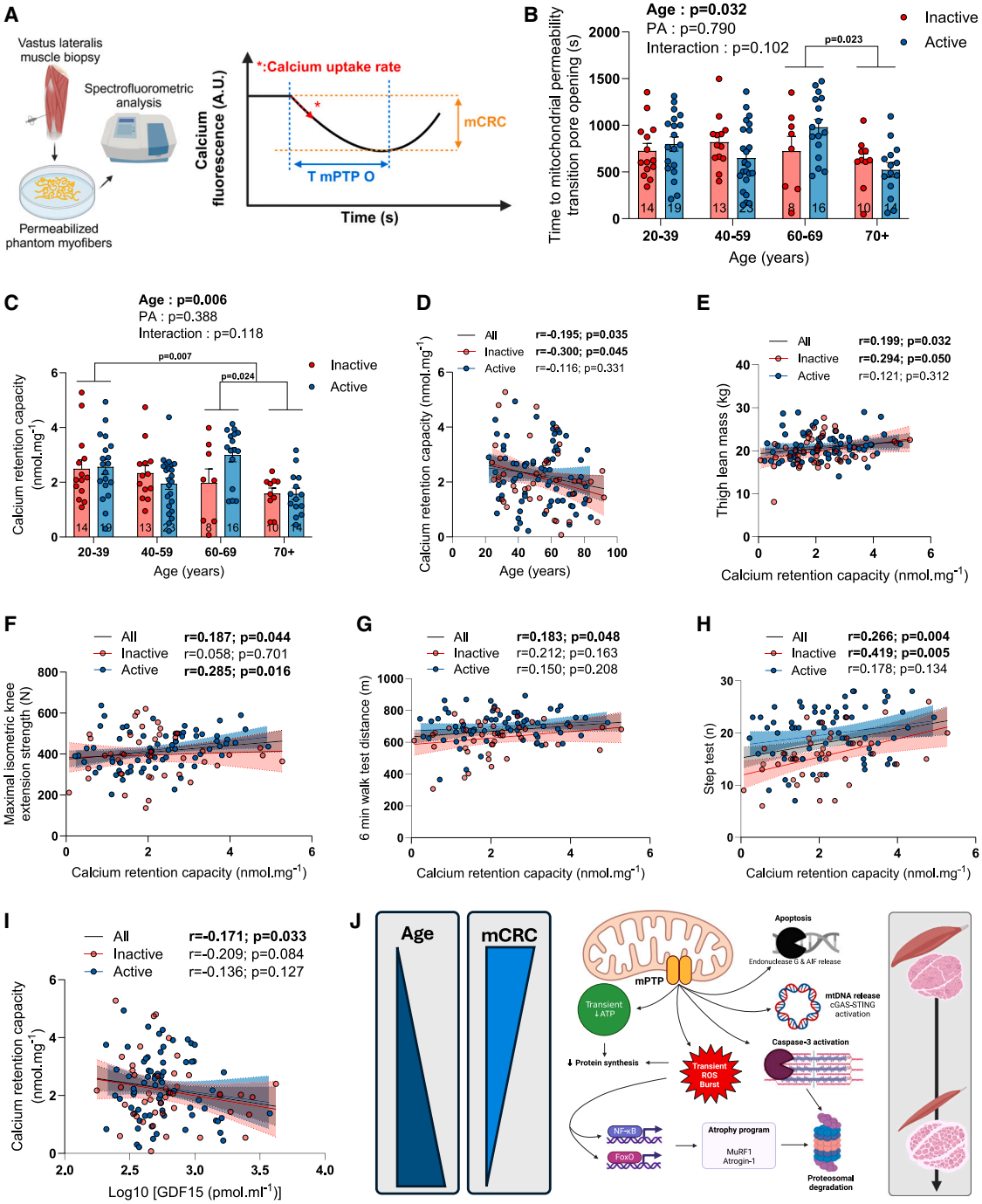

Figure 6. The impact of aging and physical activity status on skeletal muscle mitochondrial calcium handling

(A) Schematic representation of the experimental design used to assess mitochondrial calcium retention capacity (mCRC), calcium uptake rate, and time to mitochondrial permeability transition pore opening (T mPTP O) in permeabilized phantom myofibers.

(B–D) Quantification of the time to mitochondrial permeability transition pore opening (B) and mCRC (C and D) in inactive and active participants.

(E–I) Relationship between mCRC and (E) thigh lean mass, (F) maximal isometric knee extension strength, (G) distance at the 6 min walk test, (H) performance at the step test, and (I) plasma GDF15 levels (log-transformed) in our entire cohort (all) and for inactive and active participants separately. Three linear regressions are displayed in each graph to represent all, inactive, and active participants only.

(J) Schematic representation of the potential consequences of mPTP opening in muscle cells.

For group analyses, results of the two-way ANOVA are displayed above each bar graph. Tukey *post hoc* tests were performed to test differences between age groups. Data in bar graphs are presented as mean ± SEM. Differences between inactive and active participants within each age group were assessed using multiple bilateral t tests with false discovery rate (FDR) correction. Groups that do not share the same letter are significantly different. Linear regressions were

(legend continued on next page)

the mPTP may hold promise for treating age-related muscle impairments.

The present study lends strong credibility to the rising view that aging *per se* has limited impact on mitochondrial respiration.[14,17,21,23,40] Indeed, while we observed a trend for lower mitochondrial respiration in physically inactive individuals, no decline in mitochondrial respiration could be observed in physically active participants (Figure 4C). Furthermore, maximal mitochondrial respiration was positively associated with the daily number of steps in inactive participants (Figure S4C) while the daily number of steps decreased with aging (Table 1), indicating that the trend for a lower maximal mitochondrial respiration with aging in inactive individuals was consequential to reduced physical activity. Consistent with this view, it has been shown that skeletal muscle mitochondria from older adults retain high plasticity in response to variation in mechanical load. Indeed, exercise training for relatively short terms (12 weeks) can substantially increase mitochondrial content[41] and respiration in older adults.[15,42,43] Conversely, short-term disuse (10–14 days of bed rest) results in a significant decrease in mitochondrial content[44] and respiration in older adults[45,46] while 1 h of exercise per day can negate the effect of bed rest on mitochondrial bioenergetics in older adults.[46] In contrast with previous reports suggesting that aging alters mitochondrial mass-specific respiration (respiration normalized to a marker of mitochondrial content such as CS activity),[24] our data show that normalizing respiration data to CS activity not only abolished the trend for lower maximal respiration with aging in inactive participants but also abolished differences between active and inactive participants (Figures S4E and S4I). These data indicate that maximal mitochondrial mass-specific respiration is influenced by neither aging nor physical activity status. The absence of impact of physical activity status on maximal mitochondrial mass-specific respiration is consistent with a recent report in humans showing that differences in mitochondrial respiration seen between untrained, recreationally active and active-to-elite runners are abolished when normalized to mitochondrial volume or cristae density.[47]

The absence of a change in mitochondrial fatty acid oxidation with age is also worth highlighting (Figures 4D, 4E, and S4H), especially when considering that fatty acids are important mitochondrial substrates at rest and during low-intensity contractile activities, intensities most often used during activities of daily living. In contrast with previous studies that have reported data indicating mitochondrial uncoupling with muscle aging,[17,48,49] the higher ACR values seen in the present and relatively large cohort using complex I substrates (Figure S4D), and the absence of differences in ACR values when using lipids as substrates (Figure S4F), indicate that muscle mitochondrial coupling efficiency is preserved with aging in humans. This view is in line with studies in rodents and humans that have reported no decrease in the ATP/O ratio (the most direct measure of mitochondrial coupling) in aged hindlimb skeletal muscles.[40,49,50] Taken altogether, the data presented herein reinforce the necessity of considering physical activity when assessing muscle mitochondrial function, a requirement that likely extends to many other, if not all, aspects of muscle biology. Consideration related to physical activity (or lack of thereof) might also, at least in part, explain why mitochondrial respiration and content are often found impaired in old animal models of aging,[49–53] albeit not always,[54] as ambulatory activity was shown to decrease with aging in rodents.[55,56] Importantly, and as reported in other studies,[12,25,31] we also found in our cohort positive associations between mitochondrial respiration, muscle mass, strength, and power as well as physical performance (Figure S5). While our data indicate that a decrease in mitochondrial respiration is unlikely to drive the loss of muscle mass and function occurring during normal, healthy aging, they nonetheless indicate that strategies boosting muscle mitochondrial function are likely to be beneficial to the health status of older adults. The association between maximal mitochondrial respiration and plasma GDF15 levels (a stress-responsive metabokine/mitokine elevated in aging and aging-related diseases[34]), particularly evident in inactive participants, further strengthens this view.

An increase in mitochondrial ROS production is often portrayed as a mechanism driving the muscle aging process.[16] The data presented herein seriously challenge this view. Indeed, notwithstanding the use of many substrates and inhibitors of the mitochondrial oxidative phosphorylation, we did not see any effect of aging on mitochondrial H_2O_2 emission (Figures 5 and S6), a widely used surrogate measure of mitochondrial ROS production.[17,40] Even when H_2O_2 emission rates were normalized to the rate of oxygen consumption, a normalization that would reveal intrinsic alteration in ROS generation, no impact of aging was observed (Figure S7). Physically active individuals, while clearly displaying greater physical performances from adulthood to old age, even displayed greater H_2O_2 emission compared to their inactive counterparts (Figures 5 and S6). These data indicate that an increase in ROS production by the mitochondrial electron transfer system is highly unlikely to contribute to the aging-related loss of muscle mass and function in independently living men. Further strengthening this view, no negative association between mitochondrial H_2O_2 emission and muscle mass, function, and physical performance was observed in the present study (Figures S8 and S9). Our study, therefore, extends and supports previous studies that have also reported that mitochondrial ROS production is unchanged with muscle aging.[17,40,54,57] This view is also in line with previous reports that have found that long-term supplementation with the mitochondria-targeted antioxidants mitoquinone and SS-31 failed to rescue sarcopenia in rodents,[58,59] while mice deficient for Manganese SuperOxide dismutase (MnSOD), an antioxidant enzyme located in the mitochondrial matrix, do not develop muscle atrophy with aging.[60]

The present study also details the impact of aging and physical activity on skeletal muscle composition. Indeed, the trend for an increase in the proportion of type I fibers in inactive individuals

performed to assess associations between age and variables of interest in the entire cohort (all) and for inactive and active participants separately. Pearson correlation coefficients (r) and *p* values are displayed above each scatterplot. For two-way ANOVA, *post hoc* testing, and regression analyses, $p < 0.05$ was considered statistically significant. For FDR analyses, $q < 0.05$ was considered statistically significant. *, $q < 0.05$. (A) and (J) were created with BioRender.com. See also Figures S11–S13.

(Figure 3D) is somewhat in line with data published by Lexell et al. over 3 decades ago.[26] Interestingly, such a trend was not observed in active participants and indicates a preservation of their fiber type II/I ratio. Consistent with previously published data,[23] the analyses of MHC type IIa and type IIx positive myofibers (Figures 3E–3H) revealed that type IIa fibers seem particularly sensitive to aging as the proportion of pure type IIa fibers declined in both active and inactive participants. Further solidifying this view, a decrease in type IIa fiber CSA with aging was observed in active participants, albeit this observation contrasts with previously published data.[23] Combined with the trend for an increase in the proportion of type I fibers in our inactive group, this decrease in the proportion of type IIa fibers suggests a transition from type IIa to type I fibers in inactive individuals (Figure 3). In contrast, the decrease in the proportion of type IIa fibers in active participants combined with an increase in the proportion of type IIa/IIx fibers indicates remodeling within the type II fibers category with aging in physically active individuals (Figure 3). Based on data showing that exercise can improve the integrity of neuromuscular junctions (NMJs) in aged mice,[61] it is tempting to speculate that these divergent phenotypic changes seen in physically active compared to physically inactive participants might reflect a protective impact of physical activity against alterations in NMJ integrity in humans. While speculative at this stage, it should be noted that we employed an improved human muscle biopsy method to increase the probability of collecting NMJ.[62] Immunohistological analyses on samples collected during the present study are underway and should allow us to get a better understanding of the effect of aging and physical activity on NMJ integrity in humans. The aging-related increase in intermuscular fat content is another important finding of the present study (Figures 2H and 2I), as accumulating evidence positions intermuscular adipose tissue as an important player in the aging-related deterioration of skeletal muscles.[63] Our data also indicate that physical activity provides partial protection against this aging-related increase in intermuscular fat content (Figures 2H and 2I).

Another important aspect of our work was to determine the impact of physical activity on mitochondrial calcium handling across the adult lifespan. By exposing permeabilized myofibers to a calcium challenge, we found that mCRC declines with aging independently of physical activity status (Figures 6B and 6C). This finding is in line with previous studies that have reported a decline in mCRC with aging in recreationally active older adults[17] and even in master athletes.[64] When mCRC is exceeded, opening of the mPTP ensues. Our data support previous findings[17] indicating that the time to mPTP opening was reduced with aging (Figure 6C). These reductions in mCRC and time to mPTP opening demonstrate that muscle aging in humans is associated with mPTP sensitization (Figures 6B–6D). Our data indicate that the aging-related decline in mCRC and mPTP accelerates after 60 (Figures S11A and S11B). Further highlighting the biological significance of these findings, we also report that mCRC is correlated with biologically and clinically relevant measures of muscle and physical function as well as with the stress-responsive metabokine/mitokine GDF15 (Figures 6E–6I). The fact that physical activity does not protect against the aging-related decline in mCRC and mPTP opening indicate that impaired calcium handling may be a mechanism driving muscle aging as even physically active individuals display aging-related muscle atrophy and weakness (Figure 6). The aging-related alterations in calcium homeostasis that were reported in aged skeletal muscles, which include an increase in resting cytosolic calcium concentration[65–68] and reduced sarcoplasmic reticulum calcium uptake,[69] are likely to synergize with a reduced mCRC and facilitate mPTP opening *in vivo*. Moreover, it was previously reported that the proportion of endonuclease G-positive myonuclei, a nuclease involved in apoptosis normally sequestered in the intermembrane space of mitochondria and released upon mPTP opening, increases with aging in both rodent and human skeletal muscles.[17,70] Available data in rodents also provide strong support for an aging-related alteration of mCRC and mPTP function.[18,30,53] Similarly, there is solid evidence that pro-apoptotic pathways downstream of mPTP opening are activated in aged rodent skeletal muscles.[51,70,71] Since resistance training was shown to partially attenuate the aging-related decrease in sarcoplasmic reticulum calcium uptake,[69] one could speculate that physical activity might maintain a cytosolic environment that decreases the probability of mPTP opening despite reduced mCRC in active individuals. Such preservation of the mitochondrial milieu might explain the partial protection conferred by physical activity on physical performance with aging. Several apoptosis-independent events could also link the aging-related sensitization of mPTP reported herein to altered muscle mass and function. Indeed, cytochrome *c* release upon mPTP opening leads to an increase in proteasomal activity secondary to caspase-3 activation.[72] mPTP opening can also cause a transient burst in ROS production,[73] which may stimulate the atrophy program through the activation of the Forkhead box O (FoxO) transcription factor family.[74,75] mPTP opening can also result in mitochondrial DNA release[76,77] and consequential activation of the cGAS (cyclic GMP-AMP Synthase) - STING (STimulator of InterferoN Genes) - NLRP3 (NOD-, LRR and pyrin domain-containing 3) inflammasome pathway, which was linked to upregulation of key ubiquitin ligases in the muscle atrophy program[78,79] (Figure 6J).

Collectively, the data presented in the present article indicate that intrinsic changes in mitochondrial respiration and ROS production are highly unlikely to drive the normal (non-pathological) muscle aging process. Our findings also strengthen the literature positioning physical activity as a powerful stimulus to improve mitochondrial energetics throughout the human adult lifespan. Furthermore, our results position altered mitochondrial calcium handling and sensitized mPTP as putative key events contributing to muscle atrophy and weakness that occur in human aging (Figure 6J). Considering the presented data, a paradigm shift in a field overwhelmingly focused on mitochondrial bioenergetics may be needed. Finally, our results place mitochondrial calcium handling and the mPTP as potential therapeutic targets to treat the aging-related loss of muscle mass and function. Further studies will be required to test this exciting research avenue.

Limitations of the study

Our study has some limitations. First, only male participants were enrolled. Due to the large sample size that the present study required and limited budget availability, we decided to focus our study on the sex with the most linear trajectory of neuromuscular aging.[80] However, whether or not these findings are translatable

to female participants remains to be established. Second, the present study enrolled only relatively healthy community-dwelling older adults as participants. Most older adults enrolled herein displayed relatively high physical performance, including those in the inactive group. In many ways, most of them matched the definition of successful aging.[81] The magnitude and severity of mitochondrial changes with aging reported in the present study might therefore differ during states of pathological aging. Third, the cross-sectional design of our study is also limiting, preventing us from establishing a causal link between aging-related changes in mCRC and mPTP function with muscle weakness and reduced physical performance. Fourth, 138 of our 139 participants are of high socioeconomic status, which may not fully represent the diversity of the broader population.

RESOURCE AVAILABILITY

Lead contact

Requests for further information should be directed to and will be fulfilled by the lead contact, Gilles Gouspillou (gouspillou.gilles@uqam.ca).

Materials availability

This study did not generate new materials or new unique reagents.

Data and code availability

- The data reported in this paper will be shared by the lead contact upon request.
- This paper does not report original code.
- Any additional information required to reanalyze the data reported in this paper is available from the lead contact upon request.

ACKNOWLEDGMENTS

We are grateful to all study participants who donated their time and tissues. We sincerely thank Monica Tanase and Manon Dargegen for their technical assistance during muscle biopsies and for histological analyses. We thank Didier Brassard, Kelsey Dancause, and Jill Vandermeerschen for insightful discussions on statistical analyses. We are grateful to the CERMO-FC for granting us access to its Cellular and Imaging Analyses and Biophysics and Biomolecular Screening platforms. This work was funded by a Canadian Institutes of Health Research (CIHR) project grant awarded to G.G., P.G., M.A.-L., M.B., J.A.M., and R.R. (CIHR #417022) and a Natural Sciences and Engineering Research Council of Canada (NSERC) discovery grant awarded to G.G. (RGPIN-2021-03724). G.G. is supported by a chercheur-boursier Junior 2 salary award from the Fonds de recherche du Québec en Santé (FRQS-297877). M.A.-L. is supported by a Tier 1 Canada Research Chair. M.C. was supported by a postdoctoral fellowship from the FRQS. V.M. is supported by a doctoral scholarship from the FRQS.

AUTHOR CONTRIBUTIONS

M.C., V.M., P.G., M.A.-L., M.B., R.R., J.A.M., and G.G. designed the research. P.G., M.A.-L., M.B., R.R., J.A.M., and G.G. secured funding. M.C., V.M., R.H., J.G., J.-P.L.-G., J.A.M., C.T., Q.H., M.P., and G.G. performed the experiments. All authors contributed to data analysis and interpretation. M.C., V.M., and G.G. wrote the original draft with inputs from all authors. All authors read, edited, and approved the manuscript.

DECLARATION OF INTERESTS

The authors declare no competing interests.

STAR★METHODS

Detailed methods are provided in the online version of this paper and include the following:

- KEY RESOURCES TABLE
- EXPERIMENTAL MODEL AND STUDY PARTICIPANT DETAILS
- METHOD DETAILS
  - Physical activity assessment
  - Anthropometric data and body composition
  - Assessment of muscle composition using *p*-QCT
  - Assessment of physical performance
  - Assessment of muscle strength and power
  - Skeletal muscle biopsies
  - Preparation of permeabilized muscle fibers for *in situ* assessment of mitochondrial function
  - Assessment of mitochondrial respiration
  - Assessment of mitochondrial H_2O_2 emission
  - Assessment of mPTP sensitivity to calcium
  - Assessment of citrate synthase activity
  - Histology analyses
  - General blood biochemistry
  - Quantification of circulating GDF15 level
- QUANTIFICATION AND STATISTICAL ANALYSIS

SUPPLEMENTAL INFORMATION

Supplemental information can be found online at https://doi.org/10.1016/j.xcrm.2025.101968.

Received: July 16, 2024
Revised: November 5, 2024
Accepted: January 20, 2025
Published: February 10, 2025

REFERENCES

1. Cruz-Jentoft, A.J., Baeyens, J.P., Bauer, J.M., Boirie, Y., Cederholm, T., Landi, F., Martin, F.C., Michel, J.P., Rolland, Y., Schneider, S.M., et al. (2010). Sarcopenia: European consensus on definition and diagnosis: Report of the European Working Group on Sarcopenia in Older People. Age Ageing *39*, 412–423. https://doi.org/10.1093/ageing/afq034.
2. Rosenberg, I.H. (2011). Sarcopenia: origins and clinical relevance. Clin. Geriatr. Med. *27*, 337–339. https://doi.org/10.1016/j.cger.2011.03.003.
3. Gouspillou, G., Picard, M., Godin, R., Burelle, Y., and Hepple, R.T. (2013). Role of peroxisome proliferator-activated receptor gamma coactivator 1-alpha (PGC-1alpha) in denervation-induced atrophy in aged muscle: facts and hypotheses. Longev. Healthspan *2*, 13. https://doi.org/10.1186/2046-2395-2-13.
4. Janssen, I., Heymsfield, S.B., and Ross, R. (2002). Low relative skeletal muscle mass (sarcopenia) in older persons is associated with functional impairment and physical disability. J. Am. Geriatr. Soc. *50*, 889–896.
5. Janssen, I., Baumgartner, R.N., Ross, R., Rosenberg, I.H., and Roubenoff, R. (2004). Skeletal muscle cutpoints associated with elevated physical disability risk in older men and women. Am. J. Epidemiol. *159*, 413–421.
6. Santilli, V., Bernetti, A., Mangone, M., and Paoloni, M. (2014). Clinical definition of sarcopenia. Clin. Cases Miner. Bone Metab. *11*, 177–180.
7. Janssen, I., Shepard, D.S., Katzmarzyk, P.T., and Roubenoff, R. (2004). The healthcare costs of sarcopenia in the United States. J. Am. Geriatr. Soc. *52*, 80–85.
8. Leduc-Gaudet, J.P., Hussain, S.N.A., Barreiro, E., and Gouspillou, G. (2021). Mitochondrial Dynamics and Mitophagy in Skeletal Muscle Health and Aging. Int. J. Mol. Sci. *22*, 8179. https://doi.org/10.3390/ijms22158179.

9. Coen, P.M., Musci, R.V., Hinkley, J.M., and Miller, B.F. (2018). Mitochondria as a Target for Mitigating Sarcopenia. Front. Physiol. *9*, 1883. https://doi.org/10.3389/fphys.2018.01883.

10. Ferri, E., Marzetti, E., Calvani, R., Picca, A., Cesari, M., and Arosio, B. (2020). Role of Age-Related Mitochondrial Dysfunction in Sarcopenia. Int. J. Mol. Sci. *21*, 5236. https://doi.org/10.3390/ijms21155236.

11. Bellanti, F., Lo Buglio, A., and Vendemiale, G. (2021). Mitochondrial Impairment in Sarcopenia. Biology *10*, 31. https://doi.org/10.3390/biology10010031.

12. Tian, Q., Mitchell, B.A., Zampino, M., Fishbein, K.W., Spencer, R.G., and Ferrucci, L. (2022). Muscle mitochondrial energetics predicts mobility decline in well-functioning older adults: The baltimore longitudinal study of aging. Aging Cell *21*, e13552. https://doi.org/10.1111/acel.13552.

13. Picca, A., Calvani, R., Bossola, M., Allocca, E., Menghi, A., Pesce, V., Lezza, A.M.S., Bernabei, R., Landi, F., and Marzetti, E. (2018). Update on mitochondria and muscle aging: all wrong roads lead to sarcopenia. Biol. Chem. *399*, 421–436. https://doi.org/10.1515/hsz-2017-0331.

14. Distefano, G., Standley, R.A., Zhang, X., Carnero, E.A., Yi, F., Cornnell, H.H., and Coen, P.M. (2018). Physical activity unveils the relationship between mitochondrial energetics, muscle quality, and physical function in older adults. J. Cachexia Sarcopenia Muscle *9*, 279–294. https://doi.org/10.1002/jcsm.12272.

15. Grevendonk, L., Connell, N.J., McCrum, C., Fealy, C.E., Bilet, L., Bruls, Y.M.H., Mevenkamp, J., Schrauwen-Hinderling, V.B., Jörgensen, J.A., Moonen-Kornips, E., et al. (2021). Impact of aging and exercise on skeletal muscle mitochondrial capacity, energy metabolism, and physical function. Nat. Commun. *12*, 4773. https://doi.org/10.1038/s41467-021-24956-2.

16. Lei, Y., Gan, M., Qiu, Y., Chen, Q., Wang, X., Liao, T., Zhao, M., Chen, L., Zhang, S., Zhao, Y., et al. (2024). The role of mitochondrial dynamics and mitophagy in skeletal muscle atrophy: from molecular mechanisms to therapeutic insights. Cell. Mol. Biol. Lett. *29*, 59. https://doi.org/10.1186/s11658-024-00572-y.

17. Gouspillou, G., Sgarioto, N., Kapchinsky, S., Purves-Smith, F., Norris, B., Pion, C.H., Barbat-Artigas, S., Lemieux, F., Taivassalo, T., Morais, J.A., et al. (2014). Increased sensitivity to mitochondrial permeability transition and myonuclear translocation of endonuclease G in atrophied muscle of physically active older humans. FASEB J. *28*, 1621–1633. https://doi.org/10.1096/fj.13-242750.

18. Hepple, R.T. (2014). Mitochondrial involvement and impact in aging skeletal muscle. Front. Aging Neurosci. *6*, 211. https://doi.org/10.3389/fnagi.2014.00211.

19. Affourtit, C., and Carré, J.E. (2024). Mitochondrial involvement in sarcopenia. Acta Physiol. *240*, e14107. https://doi.org/10.1111/apha.14107.

20. Lee, M.J.C., Saner, N.J., Ferri, A., García-Domínguez, E., Broatch, J.R., and Bishop, D.J. (2024). Delineating the contribution of ageing and physical activity to changes in mitochondrial characteristics across the lifespan. Mol. Aspects Med. *97*, 101272. https://doi.org/10.1016/j.mam.2024.101272.

21. Distefano, G., Standley, R.A., Dubé, J.J., Carnero, E.A., Ritov, V.B., Stefanovic-Racic, M., Toledo, F.G.S., Piva, S.R., Goodpaster, B.H., and Coen, P.M. (2017). Chronological Age Does not Influence Ex-vivo Mitochondrial Respiration and Quality Control in Skeletal Muscle. J. Gerontol. A Biol. Sci. Med. Sci. *72*, 535–542. https://doi.org/10.1093/gerona/glw102.

22. Qiao, Y.S., Blackwell, T.L., Cawthon, P.M., Coen, P.M., Cummings, S.R., Distefano, G., Farsijani, S., Forman, D.E., Goodpaster, B.H., Kritchevsky, S.B., et al. (2024). Associations of accelerometry-measured and self-reported physical activity and sedentary behavior with skeletal muscle energetics: The Study of Muscle, Mobility and Aging (SOMMA). J. Sport Health Sci. *13*, 621–630. https://doi.org/10.1016/j.jshs.2024.02.001.

23. St-Jean-Pelletier, F., Pion, C.H., Leduc-Gaudet, J.P., Sgarioto, N., Zovilé, I., Barbat-Artigas, S., Reynaud, O., Alkaterji, F., Lemieux, F.C., Grenon, A., et al. (2017). The impact of ageing, physical activity, and pre-frailty on skeletal muscle phenotype, mitochondrial content, and intramyocellular lipids in men. J. Cachexia Sarcopenia Muscle *8*, 213–228. https://doi.org/10.1002/jcsm.12139.

24. Short, K.R., Bigelow, M.L., Kahl, J., Singh, R., Coenen-Schimke, J., Raghavakaimal, S., and Nair, K.S. (2005). Decline in skeletal muscle mitochondrial function with aging in humans. Proc. Natl. Acad. Sci. USA *102*, 5618–5623. https://doi.org/10.1073/pnas.0501559102.

25. Gonzalez-Freire, M., Scalzo, P., D'Agostino, J., Moore, Z.A., Diaz-Ruiz, A., Fabbri, E., Zane, A., Chen, B., Becker, K.G., Lehrmann, E., et al. (2018). Skeletal muscle ex vivo mitochondrial respiration parallels decline in vivo oxidative capacity, cardiorespiratory fitness, and muscle strength: The Baltimore Longitudinal Study of Aging. Aging Cell *17*, 1. https://doi.org/10.1111/acel.12725.

26. Lexell, J., Taylor, C.C., and Sjöström, M. (1988). What is the cause of the ageing atrophy? Total number, size and proportion of different fiber types studied in whole vastus lateralis muscle from 15- to 83-year-old men. J. Neurol. Sci. *84*, 275–294. https://doi.org/10.1016/0022-510x(88)90132-3.

27. Murach, K.A., Dungan, C.M., Kosmac, K., Voigt, T.B., Tourville, T.W., Miller, M.S., Bamman, M.M., Peterson, C.A., and Toth, M.J. (2019). Fiber typing human skeletal muscle with fluorescent immunohistochemistry. J. Appl. Physiol. *127*, 1632–1639. https://doi.org/10.1152/japplphysiol.00624.2019.

28. Momenzadeh, A., Jiang, Y., Kreimer, S., Teigen, L.E., Zepeda, C.S., Haghani, A., Mastali, M., Song, Y., Hutton, A., Parker, S.J., et al. (2023). Complete Workflow for High Throughput Human Single Skeletal Muscle Fiber Proteomics. Preprint at bioRxiv. https://doi.org/10.1101/2023.02.23.529600.

29. Murias, J.M., Kowalchuk, J.M., Ritchie, D., Hepple, R.T., Doherty, T.J., and Paterson, D.H. (2011). Adaptations in Capillarization and Citrate Synthase Activity in Response to Endurance Training in Older and Young Men. J. Gerontol. A Biol. Sci. Med. Sci. *66*, 957–964. https://doi.org/10.1093/gerona/glr096.

30. Picard, M., Ritchie, D., Wright, K.J., Romestaing, C., Thomas, M.M., Rowan, S.L., Taivassalo, T., and Hepple, R.T. (2010). Mitochondrial functional impairment with aging is exaggerated in isolated mitochondria compared to permeabilized myofibers. Aging Cell *9*, 1032–1046. https://doi.org/10.1111/j.1474-9726.2010.00628.x.

31. Coen, P.M., Jubrias, S.A., Distefano, G., Amati, F., Mackey, D.C., Glynn, N.W., Manini, T.M., Wohlgemuth, S.E., Leeuwenburgh, C., Cummings, S.R., et al. (2013). Skeletal muscle mitochondrial energetics are associated with maximal aerobic capacity and walking speed in older adults. J. Gerontol. A Biol. Sci. Med. Sci. *68*, 447–455. https://doi.org/10.1093/gerona/gls196.

32. Picard, M., Csukly, K., Robillard, M.E., Godin, R., Ascah, A., Bourcier-Lucas, C., and Burelle, Y. (2008). Resistance to Ca2+-induced opening of the permeability transition pore differs in mitochondria from glycolytic and oxidative muscles. Am. J. Physiol. Regul. Integr. Comp. Physiol. *295*, R659–R668. https://doi.org/10.1152/ajpregu.90357.2008.

33. Jena, J., García-Peña, L.M., and Pereira, R.O. (2023). The roles of FGF21 and GDF15 in mediating the mitochondrial integrated stress response. Front. Endocrinol. *14*, 1264530. https://doi.org/10.3389/fendo.2023.1264530.

34. Conte, M., Giuliani, C., Chiariello, A., Iannuzzi, V., Franceschi, C., and Salvioli, S. (2022). GDF15, an emerging key player in human aging. Ageing Res. Rev. *75*, 101569. https://doi.org/10.1016/j.arr.2022.101569.

35. Chung, H.K., Ryu, D., Kim, K.S., Chang, J.Y., Kim, Y.K., Yi, H.S., Kang, S.G., Choi, M.J., Lee, S.E., Jung, S.B., et al. (2017). Growth differentiation factor 15 is a myomitokine governing systemic energy homeostasis. J. Cell Biol. *216*, 149–165. https://doi.org/10.1083/jcb.201607110.

36. Liu, H., Huang, Y., Lyu, Y., Dai, W., Tong, Y., and Li, Y. (2021). GDF15 as a biomarker of ageing. Exp. Gerontol. *146*, 111228. https://doi.org/10.1016/j.exger.2021.111228.

37. Chiariello, A., Conte, G., Rossetti, L., Trofarello, L., Salvioli, S., and Conte, M. (2024). Different roles of circulating and intramuscular GDF15 as

markers of skeletal muscle health. Front. Endocrinol. *15*, 1404047. https://doi.org/10.3389/fendo.2024.1404047.

38. Alcazar, J., Frandsen, U., Prokhorova, T., Kamper, R.S., Haddock, B., Aagaard, P., and Suetta, C. (2021). Changes in systemic GDF15 across the adult lifespan and their impact on maximal muscle power: the Copenhagen Sarcopenia Study. J. Cachexia Sarcopenia Muscle *12*, 1418–1427. https://doi.org/10.1002/jcsm.12823.
39. Kent-Braun, J.A., and Ng, A.V. (2000). Skeletal muscle oxidative capacity in young and older women and men. J. Appl. Physiol. *89*, 1072–1078. https://doi.org/10.1152/jappl.2000.89.3.1072.
40. Zhang, X., Kunz, H.E., Gries, K., Hart, C.R., Polley, E.C., and Lanza, I.R. (2021). Preserved skeletal muscle oxidative capacity in older adults despite decreased cardiorespiratory fitness with ageing. J. Physiol. *599*, 3581–3592. https://doi.org/10.1113/JP281691.
41. Marcangeli, V., Youssef, L., Dulac, M., Carvalho, L.P., Hajj-Boutros, G., Reynaud, O., Guegan, B., Buckinx, F., Gaudreau, P., Morais, J.A., et al. (2022). Impact of high-intensity interval training with or without l-citrulline on physical performance, skeletal muscle, and adipose tissue in obese older adults. J. Cachexia Sarcopenia Muscle *13*, 1526–1540. https://doi.org/10.1002/jcsm.12955.
42. Robinson, M.M., Dasari, S., Konopka, A.R., Johnson, M.L., Manjunatha, S., Esponda, R.R., Carter, R.E., Lanza, I.R., and Nair, K.S. (2017). Enhanced Protein Translation Underlies Improved Metabolic and Physical Adaptations to Different Exercise Training Modes in Young and Old Humans. Cell Metab. *25*, 581–592. https://doi.org/10.1016/j.cmet.2017.02.009.
43. Holloway, G.P., Holwerda, A.M., Miotto, P.M., Dirks, M.L., Verdijk, L.B., and van Loon, L.J.C. (2018). Age-Associated Impairments in Mitochondrial ADP Sensitivity Contribute to Redox Stress in Senescent Human Skeletal Muscle. Cell Rep. *22*, 2837–2848. https://doi.org/10.1016/j.celrep.2018.02.069.
44. Buso, A., Comelli, M., Picco, R., Isola, M., Magnesa, B., Pišot, R., Rittweger, J., Salvadego, D., Šimunič, B., Grassi, B., and Mavelli, I. (2019). Mitochondrial Adaptations in Elderly and Young Men Skeletal Muscle Following 2 Weeks of Bed Rest and Rehabilitation. Front. Physiol. *10*, 474. https://doi.org/10.3389/fphys.2019.00474.
45. Standley, R.A., Distefano, G., Trevino, M.B., Chen, E., Narain, N.R., Greenwood, B., Kondakci, G., Tolstikov, V.V., Kiebish, M.A., Yu, G., et al. (2020). Skeletal Muscle Energetics and Mitochondrial Function Are Impaired Following 10 Days of Bed Rest in Older Adults. J. Gerontol. A Biol. Sci. Med. Sci. *75*, 1744–1753. https://doi.org/10.1093/gerona/glaa001.
46. Dulac, M., Hajj-Boutros, G., Sonjak, V., Faust, A., Hussain, S.N.A., Chevalier, S., Dionne, I.J., Morais, J.A., and Gouspillou, G. (2024). A multimodal exercise countermeasure prevents the negative impact of head-down tilt bed rest on muscle volume and mitochondrial health in older adults. J. Physiol. *15*, ejp285897. https://doi.org/10.1113/JP285897.
47. Schytz, C.T., Ørtenblad, N., Lundby, A.K.M., Jacobs, R.A., Nielsen, J., and Lundby, C. (2024). Skeletal muscle mitochondria demonstrate similar respiration per cristae surface area independent of training status and sex in healthy humans. J. Physiol. *602*, 129–151. https://doi.org/10.1113/JP285091.
48. Amara, C.E., Shankland, E.G., Jubrias, S.A., Marcinek, D.J., Kushmerick, M.J., and Conley, K.E. (2007). Mild mitochondrial uncoupling impacts cellular aging in human muscles in vivo. Proc. Natl. Acad. Sci. USA *104*, 1057–1062. https://doi.org/10.1073/pnas.0610131104.
49. Gouspillou, G., Bourdel-Marchasson, I., Rouland, R., Calmettes, G., Biran, M., Deschodt-Arsac, V., Miraux, S., Thiaudiere, E., Pasdois, P., Detaille, D., et al. (2014). Mitochondrial energetics is impaired in vivo in aged skeletal muscle. Aging Cell *13*, 39–48. https://doi.org/10.1111/acel.12147.
50. Gouspillou, G., Bourdel-Marchasson, I., Rouland, R., Calmettes, G., Franconi, J.M., Deschodt-Arsac, V., and Diolez, P. (2010). Alteration of mitochondrial oxidative phosphorylation in aged skeletal muscle involves modification of adenine nucleotide translocator. Biochim. Biophys. Acta *1797*, 143–151. https://doi.org/10.1016/j.bbabio.2009.09.004.
51. Chabi, B., Ljubicic, V., Menzies, K.J., Huang, J.H., Saleem, A., and Hood, D.A. (2008). Mitochondrial function and apoptotic susceptibility in aging skeletal muscle. Aging Cell *7*, 2–12. https://doi.org/10.1111/j.1474-9726.2007.00347.x.
52. Jedlicka, J., Tuma, Z., Razak, K., Kunc, R., Kala, A., Proskauer Pena, S., Lerchner, T., Jezek, K., and Kuncova, J. (2022). Impact of aging on mitochondrial respiration in various organs. Physiol. Res. *71*, S227–S236. https://doi.org/10.33549/physiolres.934995.
53. Martin, C., Dubouchaud, H., Mosoni, L., Chardigny, J.M., Oudot, A., Fontaine, E., Vergely, C., Keriel, C., Rochette, L., Leverve, X., and Demaison, L. (2007). Abnormalities of mitochondrial functioning can partly explain the metabolic disorders encountered in sarcopenic gastrocnemius. Aging Cell *6*, 165–177. https://doi.org/10.1111/j.1474-9726.2007.00271.x.
54. Cefis, M., Dargegen, M., Marcangeli, V., Taherkhani, S., Dulac, M., Leduc-Gaudet, J.P., Mayaki, D., Hussain, S.N.A., and Gouspillou, G. (2024). MFN2 overexpression in skeletal muscles of young and old mice causes a mild hypertrophy without altering mitochondrial respiration and H(2)O(2) emission. Acta Physiol. *240*, e14119. https://doi.org/10.1111/apha.14119.
55. Petr, M.A., Alfaras, I., Krawcyzk, M., Bair, W.N., Mitchell, S.J., Morrell, C.H., Studenski, S.A., Price, N.L., Fishbein, K.W., Spencer, R.G., et al. (2021). A cross-sectional study of functional and metabolic changes during aging through the lifespan in male mice. Elife *10*, e62952. https://doi.org/10.7554/eLife.62952.
56. Martin, B., Ji, S., Maudsley, S., and Mattson, M.P. (2010). "Control" laboratory rodents are metabolically morbid: why it matters. Proc. Natl. Acad. Sci. USA *107*, 6127–6133. https://doi.org/10.1073/pnas.0912955107.
57. Hutter, E., Skovbro, M., Lener, B., Prats, C., Rabol, R., Dela, F., and Jansen-Durr, P. (2007). Oxidative stress and mitochondrial impairment can be separated from lipofuscin accumulation in aged human skeletal muscle. Aging Cell *6*, 245–256. https://doi.org/10.1111/j.1474-9726.2007.00282.x.
58. Sakellariou, G.K., Pearson, T., Lightfoot, A.P., Nye, G.A., Wells, N., Giakoumaki, I.I., Griffiths, R.D., McArdle, A., and Jackson, M.J. (2016). Long-term administration of the mitochondria-targeted antioxidant mitoquinone mesylate fails to attenuate age-related oxidative damage or rescue the loss of muscle mass and function associated with aging of skeletal muscle. FASEB J. *30*, 3771–3785. https://doi.org/10.1096/fj.201600450R.
59. Sakellariou, G.K., Pearson, T., Lightfoot, A.P., Nye, G.A., Wells, N., Giakoumaki, I.I., Vasilaki, A., Griffiths, R.D., Jackson, M.J., and McArdle, A. (2016). Mitochondrial ROS regulate oxidative damage and mitophagy but not age-related muscle fiber atrophy. Sci. Rep. *6*, 33944. https://doi.org/10.1038/srep33944.
60. Lustgarten, M.S., Jang, Y.C., Liu, Y., Qi, W., Qin, Y., Dahia, P.L., Shi, Y., Bhattacharya, A., Muller, F.L., Shimizu, T., et al. (2011). MnSOD deficiency results in elevated oxidative stress and decreased mitochondrial function but does not lead to muscle atrophy during aging. Aging Cell *10*, 493–505. https://doi.org/10.1111/j.1474-9726.2011.00695.x.
61. Valdez, G., Tapia, J.C., Kang, H., Clemenson, G.D., Jr., Gage, F.H., Lichtman, J.W., and Sanes, J.R. (2010). Attenuation of age-related changes in mouse neuromuscular synapses by caloric restriction and exercise. Proc. Natl. Acad. Sci. USA *107*, 14863–14868. https://doi.org/10.1073/pnas.1002220107.
62. Aubertin-Leheudre, M., Pion, C.H., Vallée, J., Marchand, S., Morais, J.A., Bélanger, M., and Robitaille, R. (2020). Improved Human Muscle Biopsy Method To Study Neuromuscular Junction Structure and Functions with Aging. J. Gerontol. A Biol. Sci. Med. Sci. *75*, 2098–2102. https://doi.org/10.1093/gerona/glz292.
63. Goodpaster, B.H., Bergman, B.C., Brennan, A.M., and Sparks, L.M. (2023). Intermuscular adipose tissue in metabolic disease. Nat. Rev. Endocrinol. *19*, 285–298. https://doi.org/10.1038/s41574-022-00784-2.
64. Spendiff, S., Vuda, M., Gouspillou, G., Aare, S., Perez, A., Morais, J.A., Jagoe, R.T., Filion, M.E., Glicksman, R., Kapchinsky, S., et al. (2016).

Denervation drives mitochondrial dysfunction in skeletal muscle of octogenarians. J. Physiol. *594*, 7361–7379. https://doi.org/10.1113/JP272487.

65. Fraysse, B., Desaphy, J.F., Rolland, J.F., Pierno, S., Liantonio, A., Giannuzzi, V., Camerino, C., Didonna, M.P., Cocchi, D., De Luca, A., and Conte Camerino, D. (2006). Fiber type-related changes in rat skeletal muscle calcium homeostasis during aging and restoration by growth hormone. Neurobiol. Dis. *21*, 372–380. https://doi.org/10.1016/j.nbd.2005.07.012.
66. Mijares, A., Allen, P.D., and Lopez, J.R. (2020). Senescence Is Associated With Elevated Intracellular Resting [Ca(2 +)] in Mice Skeletal Muscle Fibers. An in vivo Study. Front. Physiol. *11*, 601189. https://doi.org/10.3389/fphys.2020.601189.
67. Terrell, K., Choi, S., and Choi, S. (2023). Calcium's Role and Signaling in Aging Muscle, Cellular Senescence, and Mineral Interactions. Int. J. Mol. Sci. *24*, 17034. https://doi.org/10.3390/ijms242317034.
68. Andersson, D.C., Betzenhauser, M.J., Reiken, S., Meli, A.C., Umanskaya, A., Xie, W., Shiomi, T., Zalk, R., Lacampagne, A., and Marks, A.R. (2011). Ryanodine receptor oxidation causes intracellular calcium leak and muscle weakness in aging. Cell Metab. *14*, 196–207. https://doi.org/10.1016/j.cmet.2011.05.014.
69. Hunter, S.K., Thompson, M.W., Ruell, P.A., Harmer, A.R., Thom, J.M., Gwinn, T.H., and Adams, R.D. (1999). Human skeletal sarcoplasmic reticulum Ca2+ uptake and muscle function with aging and strength training. J. Appl. Physiol. *86*, 1858–1865. https://doi.org/10.1152/jappl.1999.86.6.1858.
70. Leeuwenburgh, C., Gurley, C.M., Strotman, B.A., and Dupont-Versteegden, E.E. (2005). Age-related differences in apoptosis with disuse atrophy in soleus muscle. Am. J. Physiol. Regul. Integr. Comp. Physiol. *288*, R1288–R1296. https://doi.org/10.1152/ajpregu.00576.2004.
71. Marzetti, E., Wohlgemuth, S.E., Lees, H.A., Chung, H.Y., Giovannini, S., and Leeuwenburgh, C. (2008). Age-related activation of mitochondrial caspase-independent apoptotic signaling in rat gastrocnemius muscle. Mech. Ageing Dev. *129*, 542–549. https://doi.org/10.1016/j.mad.2008.05.005.
72. Wang, X.H., Zhang, L., Mitch, W.E., LeDoux, J.M., Hu, J., and Du, J. (2010). Caspase-3 cleaves specific 19 S proteasome subunits in skeletal muscle stimulating proteasome activity. J. Biol. Chem. *285*, 21249–21257. https://doi.org/10.1074/jbc.M109.041707.
73. Wang, W., Fang, H., Groom, L., Cheng, A., Zhang, W., Liu, J., Wang, X., Li, K., Han, P., Zheng, M., et al. (2008). Superoxide flashes in single mitochondria. Cell *134*, 279–290. https://doi.org/10.1016/j.cell.2008.06.017.
74. Dodd, S.L., Gagnon, B.J., Senf, S.M., Hain, B.A., and Judge, A.R. (2010). Ros-mediated activation of NF-kappaB and Foxo during muscle disuse. Muscle Nerve *41*, 110–113. https://doi.org/10.1002/mus.21526.
75. Sandri, M., Sandri, C., Gilbert, A., Skurk, C., Calabria, E., Picard, A., Walsh, K., Schiaffino, S., Lecker, S.H., and Goldberg, A.L. (2004). Foxo transcription factors induce the atrophy-related ubiquitin ligase atrogin-1 and cause skeletal muscle atrophy. Cell *117*, 399–412. https://doi.org/10.1016/s0092-8674(04)00400-3.
76. Xian, H., Watari, K., Sanchez-Lopez, E., Offenberger, J., Onyuru, J., Sampath, H., Ying, W., Hoffman, H.M., Shadel, G.S., and Karin, M. (2022). Oxidized DNA fragments exit mitochondria via mPTP- and VDAC-dependent channels to activate NLRP3 inflammasome and interferon signaling. Immunity *55*, 1370–1385.e8. https://doi.org/10.1016/j.immuni.2022.06.007.
77. Kim, J., Kim, H.S., and Chung, J.H. (2023). Molecular mechanisms of mitochondrial DNA release and activation of the cGAS-STING pathway. Exp. Mol. Med. *55*, 510–519. https://doi.org/10.1038/s12276-023-00965-7.
78. Picca, A., Lezza, A.M.S., Leeuwenburgh, C., Pesce, V., Calvani, R., Bossola, M., Manes-Gravina, E., Landi, F., Bernabei, R., and Marzetti, E. (2018). Circulating Mitochondrial DNA at the Crossroads of Mitochondrial Dysfunction and Inflammation During Aging and Muscle Wasting Disorders. Rejuvenation Res. *21*, 350–359. https://doi.org/10.1089/rej.2017.1989.
79. Liu, Y., Bi, X., Zhang, Y., Wang, Y., and Ding, W. (2020). Mitochondrial dysfunction/NLRP3 inflammasome axis contributes to angiotensin II-induced skeletal muscle wasting via PPAR-gamma. Lab. Invest. *100*, 712–726. https://doi.org/10.1038/s41374-019-0355-1.
80. Piasecki, J., Škarabot, J., Spillane, P., Piasecki, M., and Ansdell, P. (2024). Sex Differences in Neuromuscular Aging: The Role of Sex Hormones. Exerc. Sport Sci. Rev. *52*, 54–62. https://doi.org/10.1249/JES.0000000000000335.
81. Riley, M.W. (1998). Successful aging. Gerontol. *38*, 151. https://doi.org/10.1093/geront/38.2.151.
82. Mackey, D.C., Manini, T.M., Schoeller, D.A., Koster, A., Glynn, N.W., Goodpaster, B.H., Satterfield, S., Newman, A.B., Harris, T.B., and Cummings, S.R.; Health, Aging, and Body Composition Study (2011). Validation of an armband to measure daily energy expenditure in older adults. J. Gerontol. A Biol. Sci. Med. Sci. *66*, 1108–1113. https://doi.org/10.1093/gerona/glr101.
83. Washburn, R.A., Smith, K.W., Jette, A.M., and Janney, C.A. (1993). The Physical Activity Scale for the Elderly (PASE): development and evaluation. J. Clin. Epidemiol. *46*, 153–162. https://doi.org/10.1016/0895-4356(93)90053-4.
84. ATS Committee on Proficiency Standards for Clinical Pulmonary Function Laboratories (2002). ATS statement: guidelines for the six-minute walk test. Am. J. Respir. Crit. Care Med. *166*, 111–117. https://doi.org/10.1164/ajrccm.166.1.at1102.
85. (2016). Erratum: ATS Statement: Guidelines for the Six-Minute Walk Test. Am. J. Respir. Crit. Care Med. *193*, 1185. https://doi.org/10.1164/rccm.19310erratum.
86. Berg, K.O., Wood-Dauphinee, S.L., Williams, J.I., and Maki, B. (1992). Measuring balance in the elderly: validation of an instrument. Can. J. Public Health *83*, S7–S11.
87. Chung, M.M.L., Chan, R.W.Y., Fung, Y.K., Fong, S.S.M., Lam, S.S.L., Lai, C.W.K., and Ng, S.S.M. (2014). Reliability and validity of Alternate Step Test times in subjects with chronic stroke. J. Rehabil. Med. *46*, 969–974. https://doi.org/10.2340/16501977-1877.
88. Yanagawa, N., Shimomitsu, T., Kawanishi, M., Fukunaga, T., and Kanehisa, H. (2016). Relationship between performances of 10-time-repeated sit-to-stand and maximal walking tests in non-disabled older women. J. Physiol. Anthropol. *36*, 2. https://doi.org/10.1186/s40101-016-0100-z.
89. Christopher, A., Kraft, E., Olenick, H., Kiesling, R., and Doty, A. (2021). The reliability and validity of the Timed Up and Go as a clinical tool in individuals with and without disabilities across a lifespan: a systematic review. Disabil. Rehabil. *43*, 1799–1813. https://doi.org/10.1080/09638288.2019.1682066.
90. Podsiadlo, D., and Richardson, S. (1991). The timed "Up & Go": a test of basic functional mobility for frail elderly persons. J. Am. Geriatr. Soc. *39*, 142–148. https://doi.org/10.1111/j.1532-5415.1991.tb01616.x.
91. Gouspillou, G. (2023). MitoFun: Code to analyze mitochondrial respiration, H2O2 Emission and Calcium Retention Capacity Data in Igor Pro (Wavemetrics).
92. Gouspillou, G., Sgarioto, N., Norris, B., Barbat-Artigas, S., Aubertin-Leheudre, M., Morais, J.A., Burelle, Y., Taivassalo, T., and Hepple, R.T. (2014). The relationship between muscle fiber type-specific PGC-1alpha content and mitochondrial content varies between rodent models and humans. PLoS One *9*, e103044. https://doi.org/10.1371/journal.pone.0103044.
93. Matthews, D.R., Hosker, J.P., Rudenski, A.S., Naylor, B.A., Treacher, D.F., and Turner, R.C. (1985). Homeostasis model assessment: insulin resistance and beta-cell function from fasting plasma glucose and insulin concentrations in man. Diabetologia *28*, 412–419. https://doi.org/10.1007/BF00280883.

94. Katz, A., Nambi, S.S., Mather, K., Baron, A.D., Follmann, D.A., Sullivan, G., and Quon, M.J. (2000). Quantitative insulin sensitivity check index: a simple, accurate method for assessing insulin sensitivity in humans. J. Clin. Endocrinol. Metab. *85*, 2402–2410. https://doi.org/10.1210/jcem.85.7.6661.

95. Huang, Q., Monzel, A.S., Rausser, S., Haahr, R., Devine, J., Liu, C.C., Kelly, C., Thompson, E., Kurade, M., Michelson, J., et al. (2024). Psychobiological regulation of plasma and saliva GDF15 dynamics in health and mitochondrial diseases. Preprint at bioRxiv. https://doi.org/10.1101/2024.04.19.590241.

96. Kadam, P., and Bhalerao, S. (2010). Sample size calculation. Int. J. Ayurveda Res. *1*, 55–57. https://doi.org/10.4103/0974-7788.59946.

STAR★METHODS

KEY RESOURCES TABLE

REAGENT or RESOURCE	SOURCE	IDENTIFIER
Antibodies		
Alexa Fluor 488 IgG goat anti-rabbit	Thermo Fisher Scientific	Cat# A-11008; RRID:AB_143165
Alexa Fluor 594 IgG1 (y1) goat anti-mouse	Thermo Fisher Scientific	Cat# A-21125; RRID:AB_2535767
Alexa Fluor 488 IgM goat anti-mouse	Thermo Fisher Scientific	Cat# A-21042; RRID:AB_2535711
Alexa Fluor 350 IgG2b goat anti-mouse	Thermo Fisher Scientific	Cat# A-21140; RRID:AB_2535777
mouse IgG1 monoclonal anti-MHC type IIa	DSHB	Cat# SC-71; RRID:AB_2147165
mouse IgG2b monoclonal anti-MHC type I	DSHB	Cat# BA-F8; RRID:AB_10572253
mouse IgGM monoclonal anti-MHC type IIx	DSHB	Cat# BF-F3; RRID:AB_1157897
Rabbit IgG polyclonal anti-Laminin	Milipore Sigma	Cat# L9393; RRID:AB_477163
Biological samples		
Human skeletal muscles (Vastus Lateralis)	This paper	N/A
Chemicals, peptides, and recombinant proteins		
Acetyl CoA lithium salt	Milipore Sigma	Cat# A2181, CAS: 32140-51-5
Adenosine 5-diphosphate potassium salt	Milipore Sigma	Cat# A2754, CAS: 20398-34-9
Adenosine 5′-triphosphate disodium salt hydrate (Na_2 ATP)	Milipore Sigma	Cat# A2383,CAS: 34369-07-8
Amplex Ultra Red	Thermo Fisher Scientific	Cat# A36006
Antimycin A	Milipore Sigma	Cat# A8674, CAS: 1397-94-0
Bovine Serum Albumin (BSA), fatty acid free	Milipore Sigma	Cat# A6003, CAS: 9048-46-8
Calcium Green™-5N, Hexapotassium Salt	Thermo Fisher Scientific	Cat# C3737
5,5′-dithiobis-(2-nitrobenzoic acid) (DTNB)	Milipore Sigma	Cat# D8130, CAS: 69-78-3
DL-Dithiothreitol (DTT)	Milipore Sigma	Cat# D9779, CAS: 3483-12-3
Ethylene diamine tetra acetic acid (EDTA)	Milipore Sigma	Cat# 4005, CAS: 60-00-4
Ethylene glycol-bis tetra acetic acid (EGTA)	Milipore Sigma	Cat# 03777, CAS: 67-42-5
Goat Serum	Milipore Sigma	Cat# G9023,
HEPES free acid	Biobasic	Cat# HB0264, CAS: 7365-45-9
Hydrogen peroxide	Milipore Sigma	Cat# 516813, CAS: 7722-84-1
Imidazole	Biobasic	Cat# I0005, CAS: 288-32-4
Lactobionic acid	Milipore Sigma	Cat# 153516, CAS: 96-82-2
L-Glutamic acid	Milipore Sigma	Cat# G1626, CAS: 142-47-2
L-Malic acid	Milipore Sigma	Cat# M1000, CAS: 97-67-6
Magnesium chloride solution	Milipore Sigma/Fluka analytical	Cat# 63020, CAS: 7786-30-3
MES potassium salt	Milipore Sigma	Cat# M0895, CAS: 39946-25-3
3-(N-morpholino) propane sulfonic acid (MOPS)	Milipore Sigma	Cat# 475899, CAS: 71119-22-7
2-Methylbutane	Fisher Scientific	Cat# 126470010, CAS: 78-78-4
Oligomycin	Milipore Sigma	Cat# O4876, CAS: 1404-19-9
Oxaloacetic acid	Milipore Sigma	Cat# O4126, CAS: 328-42-7
Palmitoyl-DL-carnitine chloride	Milipore Sigma	Cat# P4509, CAS: 6865-14-1
Peroxidase from horseradish (HRP)	Milipore Sigma	Cat# P8375, CAS: 9003-99-0
Phosphate buffered saline	Milipore Sigma	Cat# P4417-100Tab;
Phosphocreatine disodium salt hydrate	Milipore Sigma	Cat# P7936, CAS: 19333-65-4
Potassium chloride 99% purity	Fisher Scientific	Cat# P2173, CAS: 7447-40-7
Potassium phosphate dibasic (Pi) (HK_2O_4P)	Milipore Sigma	Cat# P3786, CAS: 7758-11-4
Potassium phosphate monobasic (H_2KO_4P)	Milipore Sigma	Cat# P5379, CAS: 7778-77-0
Prolong™ Gold	Invitrogen	Cat# P36930

(*Continued on next page*)

Continued

REAGENT or RESOURCE	SOURCE	IDENTIFIER
Saponin	Milipore Sigma	Cat# 47036, CAS: 8047-15-2
Sodium cacodylate trihydrate	Milipore Sigma	Cat# C4945, CAS: 6131-99-3
Sodium succinate dibasic hexahydrate	Milipore Sigma	Cat# S2378, CAS: 6106-21-4
Sucrose	Biobasic	Cat# S2560, CAS: 57-50-1
Superoxide Dismutase (SOD)	Milipore Sigma	Cat# S7446, CAS: 9054-89-1
Taurine	Milipore Sigma	Cat# T0625, CAS: 107-35-7
Tragacanth	Milipore Sigma	Cat# G1128, CAS: 9000-65-1
Triethanolamine hydrochloride	Milipore Sigma	Cat# T1502, CAS: 637-39-8
Tris	BioShop	Cat# TROS001, CAS: 77-86-1
Tris (hydroxylmethyl) aminomethane (Tris)	BioShop	Cat# TROS001.1, CAS: 77-86-1
Triton X-100	Milipore Sigma	Cat# X100, CAS: 9036-19-5
Water deionized	Milipore Sigma	Cat# 7732-18-5
Critical commercial assays		
Cholesterol	Beckman Coulter	Cat# BAOSR6X16
C-reactive protein	Beckman Coulter	Cat# BAOSR6X99
Fructosamin	Randox	Cat# FR 3133
GDF15	R&D Systems	Cat# DGD150, SGD150
HDL	Beckman Coulter	Cat# BAOSR6X95
Insulin	Abbott	Cat# ARCHITECT Insulin 8K41
Serum glucose	Beckman Coulter	Cat# BAOSR6X21
Serum protein levels	Beckman Coulter	Cat# BAOSR6X32
Triglycerides	Beckman Coulter	Cat# BAOSR6X118
Software and algorithms		
BioRender	BioRender	https://biorender.com/; RRID:SCR_018361
CellSens 2.2	Olympus	https://www.olympus-lifescience.com/en/software/cellsens/
Clampfit 11.2	Molecular Devices	https://www.moleculardevices.com/products/axon-patch-clamp-system/acquisition-and-analysis-software/pclamp-software-suite
DatLab 7.3.0.3	Oroboros Instruments	https://www.oroboros.at/index.php/product/datlab/
Encore 2008 12.3	GE Healthcare Prodigy	https://www.gehealthcare.com/products/bone-and-metabolic-health/encore-software-platform?srsltid=AfmBOorxAQVS-eX79A9w9P0PEYaqpYguiPbRN6O_6fDXbLaxLX2nUdlY
GraphPad Prism 10.1.3	GraphPad	https://www.graphpad.com/; RRID: SCR_002798
I-control 1.9	Tecan	https://www.tecan.com/knowledge-portal/how-to-install-your-infinite-200-pro-and-i-control-software
Igor Pro 8	WaveMetrics	RRID: SCR_000325
ImageJ (for image analysis)	NIH	https://imagej.nih.gov/ij/; RRID:SCR_003070
MitoFun	(Gouspillou 2023)	https://doi.org/10.5281/zenodo.7510439
Sensewear 8.1	BodyMedia	N/A
Stratec XCT Console	Stratec	https://stratec-pqct.com/en/
Other		
Alcohol prep pads sterile	Curad	Cat# CURCA45581R1
Baxedin Pre-op chlorhexidin 0.5% and alcool 70%	Omega Laboratories	Cat# L0000003

(*Continued on next page*)

Continued

REAGENT or RESOURCE	SOURCE	IDENTIFIER
Dressing tray	Med-RX	Cat# 85-4011
Gauze Pads Sterile, 4″ × 4"	Covidien	Cat# 441412
Latex surgical gloves sterile	Ansell	Cat# 5785003
2% Lidocaïne Hydrochloride (20 mg/mL)	Teligent Canada	Cat# ALV0127AG01
Microscope Slides Superfrost Plus	Fisher Scientific	Cat# 12-550-15
Monitoring Line 48in	Medex	Cat# MX564
Needle (black) Precision Glides, 38mm, 22G	BD	Cat# 305156
Needle (blue) Precision Glides, 16mm, 25G	BD	Cat# 305122
Needle (pink) Precision Glides, 25mm, 18G	BD	Cat# 305195
Plastic Adhesive Bandage Strip, 3/4″ × 3″, Sterile, Latex-Free.	Alliance Healthcare Products	Cat# 211-018-600
Sealing Cap for Muscle Biopsy Needle	Millenium Surgical	Cat# 72-230006
Safety-Lok™ Blood Collection Set with 12 in. tubing and luer adapter 23 G x 0.75 in.	BD Vacutainer	Cat# 367283
Single use scalpel sterile	Paragon	Cat# 0086
Sterile field towel	Medicom SafeBasics	Cat# 8201
Steri-Strip Reinforced Adhesive Skin Closure,	3M	Cat# R1541
Syringe 10mL Luer-Lock	BD	Cat# BD302995
Syringe 140mL Monoject Luer-Lock Tip	Covidien	Cat# 8881114030
UCH Style Skeletal Muscle Biopsy Needle 6 mm × 120 mm 5 standard wire gauge x 4.75″	Millenium Surgical	Cat# 72-238069
Vacutainer venous blood collection tube (gold)	BD	Cat# 367986
Vacutainer venous blood collection tube with EDTA (lavender)	BD	Cat# 367861

EXPERIMENTAL MODEL AND STUDY PARTICIPANT DETAILS

Participants were recruited by advertisements in newspapers, bulletin boards, social media and through word of mouth. To be included, participants had to self-identify as a male and a man aged between 20 and 100 years old, with a BMI between 18 and 35 kg/m^2. The following exclusion criteria were used: uncontrolled metabolic disease, neurodegenerative disease, smoking more than 2 cigarettes per day, drinking more than 2 glasses of alcohol per day, taking anticoagulant medication, having a pacemaker or a metal implant. Three separate on-site visits, organized within one month, were required to complete all measurements and procedures. All participants provided informed written consent after having received information on the nature, goal, procedures, and risks associated with the study. Participants were informed to maintain their physical activity and diets habits during their participation. To investigate the impact of aging and physical activity status on our variables of interest, participants were divided in the following age groups: young middle age (20–39 yo), mature middle age (40-59yo), young older adults (60–69 yo) and older adults (70+ yo) and sub-divided in inactive and active according to their physical activity status. Socioeconomic data were not collected. Our cohort was composed of 91.4% White not Hispanic, 4.3% Arab, 2.2% Asian, 1.4% White Hispanic and 0.7% multiracial. All procedures were approved by the Ethics Committee of the *Université du Québec á Montréal* (UQÀM) (Ethic certificate number: 2020–2703). The study was conducted in the *Département des Sciences de l'activité physique* at UQÀM between February 2020 and June 2023.

METHOD DETAILS

Physical activity assessment

To estimate the status of physical activity for each participant, we combined two approaches.

(1) Objective measures using a tri-axial accelerometer (SenseWearMini Armband).[82] Participants were asked to wear the armband on the non-dominant arm for at least 3 days and ideally for 7 days. Data were taken from days where the armband was worn at least 80% of the time over 24h (≥19h and 12 min). Data were analyzed using the software Armband Sensewear 8.1.

(2) Self-reported physical activity obtained through a structured interview with a trained kinesiologist. Questions asked during the interview were derived from the physical Activity Scale for the Elderly (PASE).[83] However, participants were asked to report their usual physical activity representative of the past 5 years and not just their physical activity over 7 days.

To be deemed active, participants had to fulfill at least one of the following criteria.

(1) Engage in a minimum of 150 min per week of structured moderate to intense physical activity, ii) Achieve a daily step count of at least 10,000 steps, or iii) Maintain a MET equal to or greater than 1.6.

Aerobic training included endurance-focused activities such as running, cycling, swimming, and team sports (e.g., hockey, soccer). Resistance training included strength-focused activities such as weightlifting, powerlifting, and calisthenics.

Anthropometric data and body composition

Height (in cm) was measured using a wall-mounted height gauge (SECA 67029, Hanover, MD, USA) and mass (in kg), with an electronic scale (ADAM - GFK 660a, USA). The BMI was calculated using the following formula: Mass (kg)/Height (m).[2] DXA (GE Prodigy Lunar) was used to assess fat and lean masses. Participants were fasted for a minimum of 2 h before the DXA scan.

Assessment of muscle composition using *p*-QCT

Muscle composition was assessed using a peripheral quantitative computed tomography scan (*p*-QCT; Stratec XCT3000 STRATEC Medizintechnik GmbH, Pforzheim, Germany, Division of Orthometrix; White Plains, NY, USA). Images were taken in the lower third of the right thigh (from the right lateral epicondyle to the greater trochanter of the right femur). Acquisition parameters were the following: voxel size: 0.5 mm; speed:10 mm/s *p*-QCT images were analyzed using ImageJ software (NIH, Bethesda, Maryland, USA, https://imagej.nih.gov/ij/) with the plugin *p*-QCT.

Assessment of physical performance

Four validated tests were performed to assess physical performance as previously described Marcangeli et al.[41].

(1) 6 min walking test.[84,85] The test was performed on a 25-meter track and participants were asked to walk as much as possible during 6 min. No encouragement was received along the test. The total distance was recorded in meters.
(2) alternative step test.[86,87] Participants were placed facing toward a 20 cm height step and instructed to touch the top with the right and left foot, alternatively, as fast as possible during a 20 s period. The number of steps was recorded.
(3) "Sit to stand" test. Participants were asked to repeat standing up from a sitting position and sitting down as fast as possible for 30s with arms across their chests.[88] The time to perform 10 repetitions (10rep sit to stand) and the number of repetitions performed during 30s were recorded.
(4) "Timed Up & Go" test.[89] This test, which consists in standing from a chair, walking a 3 m distance and sitting down again,[90] was performed at a fast-paced walking speed. The time to perform this task was recorded.

Assessment of muscle strength and power

The maximal isometric knee extension strength and the maximal lower limb muscle power were evaluated as previously described.[41] Maximal isometric knee extension strength was assessed on the right leg using a strain gauge system attached to a chair (Primus RS Chair, BTE) upon which participants were seated with the knee and hip joint angles set at 135°and 90°, respectively. The knee angle was set to 135°, compared to the typical 90° to diminish the maximal joint torque that could be generated, particularly in light of generally more fragile bones in older adults. The tested leg was fixed to the lever arm at the level of the lateral malleoli on an analog strain gauge to measure strength. The highest of three maximum voluntary contractions was recorded.

Lower limb muscle power was measured on the right leg using the Nottingham Leg Extensor Power rig in a sitting position. Participants were asked to push the pedal down as hard and fast as possible, accelerating a flywheel attached to an analog to digital converter. Power was recorded for each push until a plateau/decrease was observed.

Skeletal muscle biopsies

Muscles biopsies were collected using the Biopsy Electrostimulation for Enhanced NeuroMuscular Junction Sampling (BeeNMJs) method as extensively described.[62] This approach, which allows for enrichment of NMJ in muscle biopsy samples, was selected as our overall research project was aimed at investigating the contributions of mitochondrial dysfunction and altered NMJ integrity in the human muscle aging process. Analyses of NMJ integrity are currently underway and will be part of a separate manuscript. The first step of the BeeNMJs method consists in identifying the region of the vastus lateralis with the highest NMJ density through electrostimulation.[62] Once identified, muscle biopsies were performed along the main axis of the vastus lateralis at least 2 cm away from the site with the highest NMJ density. Muscle biopsies were performed using a suction modified Bergström needle under local anesthesia (lidocaine injection). The tissue collected during the biopsy procedures was either used fresh to assess mitochondrial function, prepared for histological analyses, prepared to assess NMJ integrity or snap frozen in liquid nitrogen and stored at −80°C until use.

Preparation of permeabilized muscle fibers for *in situ* assessment of mitochondrial function

Mitochondrial function was assessed in fresh muscle biopsy samples. Once dissected, muscle biopsy samples were weighted with a precision scale and then rapidly immersed in ice-cold stabilizing buffer A (2.77 mM CaK_2 ethylene glycol-bis-(2-aminoethylether)-N,N,N,N-tetraacetic acid (EGTA), 7.23 mM K_2 EGTA, 6.56 mM $MgCl_2$, 0.5 mM dithiothreitol (DTT), 50 mM 2-(N-morpholino) ethanesulfonic acid potassium salt (K-MES), 20 mM imidazole, 20 mM taurine, 5.3 mM Na_2 ATP, and 15 mM phosphocreatine, pH 7.3). Muscle biopsy samples were separated into small fiber bundles using fine forceps under a surgical dissecting microscope (Leica S4 E, Germany). Muscle fiber bundles were incubated into a glass scintillation vial for 30 min at low rocking speed containing buffer A supplemented with 0.05 mg/mL saponin (Sigma-Aldrich) to selectively permeabilize the sarcolemma. Fiber bundles was divided in two parts, once was washed 3 times 10 min at low rocking speed in the MiR05 buffer (110 mM sucrose, 20 mM HEPES, 10 mM KH_2PO_4, 20 mM taurine, 60 mM K-lactobionate, 3 mM $MgCl_2$, 0.5 mM EGTA, 1 g/L of fatty acid free BSA, pH 7.4) to assess mitochondrial respiration and H_2O_2 emission. The other part of fiber bundles was washed 3 times 10 min at low rocking speed in the C buffer (80mM K-MES, 50mM HEPES, 20mM taurine, 0.5mM DTT, 10mM $MgCl_2$, 10mM ATP, pH 7.3) to realize mPTP analyses. All incubations were performed in vials placed on ice.

Assessment of mitochondrial respiration

Permeabilized myofibers from muscle biopsy samples were used to assess mitochondrial respiration in an Oroboros O2K high-resolution fluororespirometer (Oroboros Instruments, Austria) at 37°C in 2 mL of MiR05 buffer. Briefly, 3 to 6 mg (wet mass) of permeabilized fiber bundles were weighed and added to the respiration chambers. The following 2 protocols were used.

(1) Protocol 1 consisted in the sequential addition of the following substrates and inhibitors: 10 mM glutamate +5 mM malate (G + M), 2 mM ADP, 10 mM succinate, 1μM oligomycin and 2μM antimycin A.
(2) Protocol 2 consisted in the sequential addition of the following substrates and inhibitors: 200 μM mM palmitoyl-L-carnitine +5 mM malate, 2 mM ADP.

After mitochondrial respiration measurements, bundles were removed and placed in liquid nitrogen and stored at −80°C for the assessment of citrate synthase (CS) activity. Respiration rates were normalized as picomoles of dioxygen per second per mg of wet muscle mass. All respiration experiments were analyzed with MitoFun,[91] a homemade code to analyze mitochondrial function data in the Igor Pro 8 software (Wavemetrics, OR, USA).

Assessment of mitochondrial H_2O_2 emission

The H_2O_2 emission from myofiber bundles was assessed by monitoring the rate of H_2O_2 release using the amplex ultra red-horseradish peroxidase system. This was performed along with respiration assessment in the Oroboros O2K high-resolution fluororespirometer (Oroboros Instruments, Austria) at 37°C in 2 mL of MiR05 buffer supplemented with Amplex Ultra Red (10μM), SOD (5 U/ml), and HRP (1 U/ml). A calibration curve was generated daily using successive additions of known [H_2O_2] in absence of tissue. After mitochondrial H_2O_2 emission measurements were completed, bundles were retrieved, snap frozen in liquid nitrogen and stored at −80°C until CS activity measures. H_2O_2 emission was normalized as picomoles per second per milligram of wet muscle mass. All H_2O_2 emission experiments were analyzed with MitoFun,[91] a homemade code to analyze mitochondrial function data in the Igor Pro 8 software (Wavemetrics, OR, USA).

Assessment of mPTP sensitivity to calcium

Sensitivity to mPTP opening was assessed by determining mitochondrial CRC in the presence of a calcium challenge.[32] The high affinity for Ca^{2+} of myosin-actin-associated proteins prevents measurements of mitochondrial Ca^{2+} uptake in standard permeabilized myofibers. To overcome this limitation, phantom fibers (fibers without myosin) were prepared.[32] As mentioned earlier, fiber bundles were first permeabilized with saponin and washed 3 times in buffer C. The bundles were then incubated for 30 min with intermittent manual agitation at 4°C in buffer D (800 mM KCl, 50 mM HEPES, 20 mM taurine, 0.5 mM DTT, 10 mM $MgCl_2$, and 10 mM ATP, pH 7.3 at 4°C), a solution of high ionic force to extract myosin but which preserves mitochondrial function (phantom fibers). Bundles were finally washed 3 times in low-EGTA CRC buffer (250 mM sucrose, 10 mM Tris, 5 μM EGTA, and 10 mM 3-(*N*-morpholino) propane sulfonic acid (MOPS), pH 7.3 at 4°C) and kept on ice until use for Ca^{2+}-induced mPTP opening assays. The CRC was then determined in permeabilized phantom fibers as previously described.[17] Briefly, a muscle bundle of 3–6 mg wet mass was added to 600 μL of CRC buffer containing ~30 μM of Ca^{2+} supplemented with 5 mM glutamate, 2.5 mM malate, 10 mM inorganic phosphate (P_i), 1 μM calcium-green 5 N, and 0.5 μM oligomycin. Mitochondrial Ca^{2+} uptake was immediately followed by monitoring the decrease in extramitochondrial Ca^{2+}concentration using the fluorescent probe calcium-green 5 N (C3737, ThermoFisher). Fluorescence was detected using a spectrophotometer (Hitachi F2500, FL Solutions software) with excitation and emission detectors set at 505 and 535 nm, respectively. All measurements were performed at 37°C. Progressive uptake of Ca^{2+} by mitochondria was monitored until mitochondrial Ca^{2+} release caused by opening of the mPTP was observed as the inversion of signal. CRC was calculated as total amount of Ca^{2+} taken by mitochondria before Ca^{2+} release. Fluorescent units were converted into Ca^{2+} concentration using a standard curve obtained daily using successive addition of known Ca^{2+} concentration in the absence of sample. CRC values were expressed per milligram of wet fiber mass. The time to pore opening was also calculated as a time that mitochondria take to open the

permeability transition pore and release the Ca^{2+}, and data were expressed in seconds. All mPTP experiments were analyzed with MitoFun,[91] a homemade code to analyze mitochondrial function data in the Igor Pro 8 software (Wavemetrics, OR, USA).

Assessment of citrate synthase activity

Enzymatic activity level of the mitochondrial citrate synthase was determined spectrophotometrically on permeabilized myofibers frozen immediately after fluororespirometry and calcium retention capacity assays. Briefly, permeabilized myofibers were homogenized in 20 volumes of an extraction buffer containing 1 mM EDTA, Triethanolamine 50mM. The homogenates were centrifuged at 10,000g for 2 min at 4°C and incubated on ice for 1h. The supernatants were collected in a clean Eppendorf and CS activity was measured spectrophotometrically by detecting the increase in absorbance at 412 nm in a 96-well plate, at 30°C, using 200μL of a reaction buffer (200 mM Tris, pH 7.4) containing 2μM acetyl-CoA, 200μM 5,5′-dithiobis-(2-nitrobenzoic acid) (DTNB), 350 μM oxaloacetic acid, and 0.1% Triton X-100. The kinetic assay was performed with the M1000 TECAN multiplate reader for 2 min with repeated measures every 5 s. To calculate the CS activity, the DTNB molar extinction coefficient used was 13.6 L $mol^{-1}.cm^{-1}$. CS activity absorbance units were normalized to mg of frozen fibers.

Histology analyses

Skeletal muscle sample sectioning

Muscle biopsies samples were mounted in tragacanth (Sigma, G1128), frozen in cooled liquid isopentane, and stored at −80°C. Ten-micron thick serial cross-sections were cut in a cryostat at −20°C and mounted on lysine coated slides (Superfrost).

Assessment of muscle fiber type and size

Muscle cross-sections were immunolabelled for different MHC isoforms as previously described.[23,92] Briefly, muscle cross sections were allowed to reach room temperature, rehydrated with Phosphate Buffer solution (PBS, Sigma, 4417) and blocked with PBS containing 10% of goat serum (GS) for 45 min at room temperature. Muscle sections were then incubated for 1 h, at room temperature with the following primary antibodies mix: a mouse IgG2b monoclonal anti-MHC type I (BA-F8, 1:25, DSHB, Iowa, IA, USA), a mouse IgG1 monoclonal anti-MHC type IIa (Sc-71, 1:200, DSHB, Iowa, IA, USA), a mouse IgM monoclonal anti-MHC type IIx (6-H1, 1:25, DSHB, Iowa, IA, USA) and a rabbit IgG polyclonal anti-laminin (Sigma, L9393, 1:750) diluted in PBS containing 10% of GS. Muscle cross-sections were then washed 3 times with PBS before being incubated for 1 h with the following secondary antibodies mix diluted in PBS containing 10% of GS: Alexa Fluor 350 IgG2b goat anti-mouse (A21140), Alexa Fluor 594 IgG1 goat anti-mouse (A21125), Alexa Fluor 488 IgM goat anti-mouse (A21042) and Alexa Fluor 488 IgG goat anti-rabbit (A11008). Sections were washed 3 times in PBS and cover slipped using Prolong Gold (Invitrogen, P36930) as mounting medium. Slides were imaged using an Olympus IX83 Ultra Sonic fluorescence microscope (Olympus, Japan). Analyses of fiber type and size were performed by an experimenter blinded to the participants age and physical activity status. At least 200 fibers were manually traced per participant (average ±SD: 314 ± 86) using the ImageJ software (NIH, Bethesda, Maryland, USA, https://imagej.nih.gov/ij/).

General blood biochemistry

Fifteen mL of venous blood sample were collected after an overnight fast in BD Vacutainer SST Tube with Hemogard Closure (Gold, Dufort et Lavigne Ltée, Qc, Canada, BEC367986). Tubes were inverted 6 times and were then left at room temperature for a minimum of 30 min and maximum of 60 min for clotting. Gold tubes were then stored at 4°C, for a maximum of 4 h, before centrifugation. Gold tubes were centrifuged at 2000g for 15 min at room temperature. After centrifugation, the supernatant (serum) was collected and aliquoted into 1.5 mL Eppendorf tubes and immediately stored at −80°C until use.

Serum glucose concentrations were assessed using a coupled enzymatic assay in a Beckman Coulter AU analyzer according to the manufacturer's instructions (Beckman Coulter, BAOSR6X21). Serum insulin concentrations were assessed using the ARCHITECT Insulin assay according to the manufacturer's instructions (Abbott, ARCHITECT Insulin 8K41). Fructosamine levels were assessed using a colorimetric assay according to the manufacturer's instruction (Randox, FR 3133).Total cholesterol and HDL-cholesterol were assessed using a Beckman Coulter AU analyzer according to the manufacturer's instructions (Beckman Coulter, BAOSR6X16 and BAOSR6x95, respectively). LDL cholesterol was calculated based on HDL-cholesterol and triglycerides values as follows: LDL cholesterol = total cholesterol - HDL - (triglycerides/5). The HOMA-IR was calculated as [fasting glucose (mmol/L) x fasting insulin (pmol/L)]/135.[93] The Quantitative Insulin Sensitivity Check Index (QUICKI) 1/[log fasting insulin (μU/mL) + log glucose (mg/dL)].[94] C-reactive protein (CRP) levels were assessed using the Beckman Coulter CRP latex assay in a Beckman Coulter AU analyzer according to the manufacturer's instructions (Beckman Coulter, BAOSR6X99). Abnormally high CRP values for two participants (one in the 60–69 inactive group and one in the 70+ active group) were removed from the analyses. Triglycerides levels were assessed using a colorimetric assay in a Beckman Coulter AU analyzer according to the manufacturer's instructions (Beckman Coulter, BAOSR6X118). Serum protein levels were assessed using a colorimetric assay in a Beckman Coulter AU analyzer according to the manufacturer's instructions (Beckman Coulter, BAOSR6X32).

Quantification of circulating GDF15 level

Fifteen mL of venous blood sample were collected after an overnight fast in BD Vacutainer EDTA (ethylenediaminetetraacetic acid) Tube with BD Hemogard Closure (Lavender, Dufort et Lavigne Ltée, Qc, Canada, BEC367961). Lavender tubes were inverted 10 times and then stored at 4°C, for a maximum of 4 h, before centrifugation. Lavender tubes were centrifuged at 2000g for 15 min

at room temperature. After centrifugation, the supernatant (plasma) was collected and aliquoted into 1.5 mL Eppendorf tubes and stored at −80°C until use. Plasma GDF15 levels were quantified using a high-sensitivity ELISA kit (R&D Systems, DGD150, SGD150) as described previously.[95]

QUANTIFICATION AND STATISTICAL ANALYSIS

All statistical analyses were performed using GraphPad Prism 10.1.3. Estimation of sample sizes to detect significant differences, with an alpha error set at 0.05 and power set at 0.80, for the most relevant parameters of muscle and mitochondrial function were performed as described in[96] and based on our previously published data.[17,23] These estimations retrieved minimal sample sizes required to achieve adequate power of $n = 8$ to 10 per group. Group comparisons were performed using two-way analysis of variance (ANOVA; $p < 0.05$ were considered significant) with age and physical activity status as factors. When an age effect was observed, Tukey's multiple comparisons tests were performed to assess differences between age groups ($p < 0.05$ were considered significant). To assess whether differences were present between active and inactive participants in each age group, bilateral Student's t-tests followed by a correction using the false discovery rate (FDR) (using the two-stage step-up method of Benjamini, Krieger, and Yekutieli) was applied ($p < 0.05$ and $q < 0.05$ were considered significant). For analyses where age was considered as a continuous variable, and for all correlation analyses, simple linear regressions were performed, and Pearson r coefficients were calculated. To test whether correlations were significant, two-tailed tests were used for all correlations except for correlations involving plasma GDF15 levels which were tested with one-tailed tests. Bar graphs are presented as mean ± standard error of the mean (SEM). The exact number of participants within each group or analysis in all figures is indicated either in bar graphs or in the figure legends. Individual data are displayed in each graph.